Journal Pre-proof

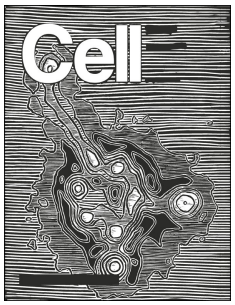

¬Post-Gastrulation Synthetic Embryos Generated Ex Utero from Mouse Naïve ESCs

Shadi Tarazi, Alejandro Aguilera-Castrejon, Carine Joubran, Nadir Ghanem, Shahd Ashouokhi, Francesco Roncato, Emilie Wildschutz, Montaser Haddad, Bernardo Oldak, Elidet Gomez-Cesar, Nir Livnat, Sergey Viukov, Dmitry Lukshtanov, Segev Naveh-Tassa, Max Rose, Suhair Hanna, Calanit Raanan, Ori Brenner, Merav Kedmi, Hadas Keren-Shaul, Tsvee Lapidot, Itay Maza, Noa Novershtern, Jacob H. Hanna

PII: S0092-8674(22)00981-3

DOI: https://doi.org/10.1016/j.cell.2022.07.028

Reference: CELL 12584

To appear in: *Cell*

Received Date: 5 June 2022

Revised Date: 8 July 2022

Accepted Date: 28 July 2022

Please cite this article as: Tarazi, S., Aguilera-Castrejon, A., Joubran, C., Ghanem, N., Ashouokhi, S., Roncato, F., Wildschutz, E., Haddad, M., Oldak, B., Gomez-Cesar, E., Livnat, N., Viukov, S., Lukshtanov, D., Naveh-Tassa, S., Rose, M., Hanna, S., Raanan, C., Brenner, O., Kedmi, M., Keren-Shaul, H., Lapidot, T., Maza, I., Novershtern, N., Hanna, J.H., ¬Post-Gastrulation Synthetic Embryos Generated Ex Utero from Mouse Naïve ESCs, *Cell* (2022), doi: https://doi.org/10.1016/j.cell.2022.07.028.

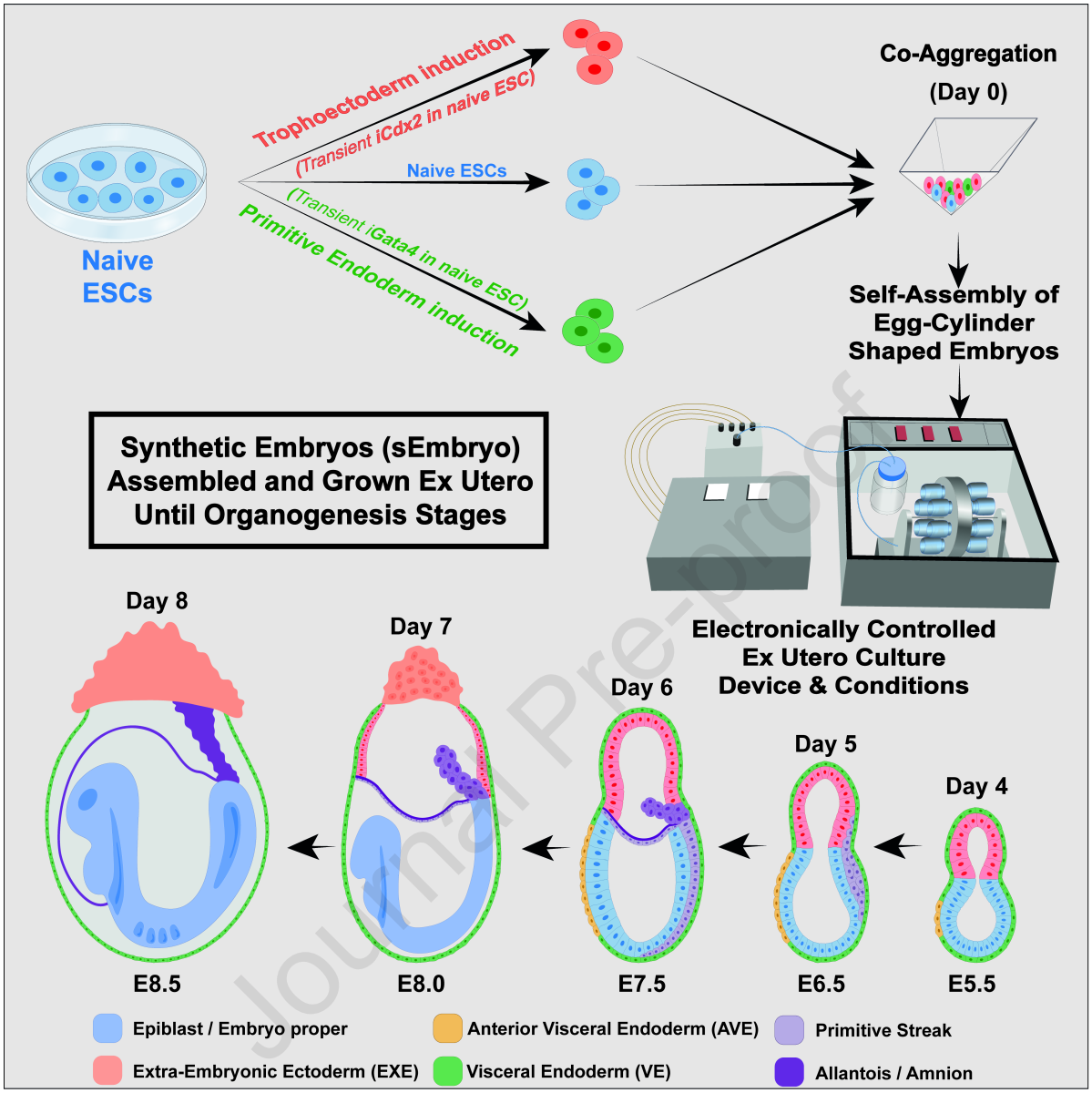

Post-Gastrulation Synthetic Embryos Generated Ex Utero from Mouse Naïve ESCs

Shadi Tarazi[1,8*], Alejandro Aguilera-Castrejon,[1,8,10*] Carine Joubran[1,8], Nadir Ghanem[2], Shahd Ashouokhi,[1] Francesco Roncato[1], Emilie Wildschutz[1], Montaser Haddad[3], Bernardo Oldak[1,] Elidet Gomez-Cesar[1], Nir Livnat,[1] Sergey Viukov[1], Dmitry Lukshtanov[1], Segev Naveh-Tassa[1], Max Rose[1], Suhair Hanna[4], Calanit Raanan[5], Ori Brenner[5], Merav Kedmi[6], Hadas Keren-Shaul[6], Tsvee Lapidot[3], Itay Maza[7,9*], Noa Novershtern[1,9,10*] & Jacob H. Hanna[1,10*@]

[1]Department of Molecular Genetics, Weizmann Institute of Science, Rehovot 76100, Israel

[2]Department of Obstetrics and Gynecology, Rambam Health Care Campus, Bruce Rappaport faculty of Medicine, Technion, Haifa, Israel

[3]Department of Immunology and Regenerative Biology, Weizmann Institute of Science, Rehovot 76100, Israel

[4]Department of Pediatrics, Rambam Health Care Campus, Technion, Haifa, Israel

[5]Department of Veterinary Resources, Weizmann Institute of Science, Rehovot 76100, Israel

[6]Department of Life Sciences Core Facilities, Weizmann Institute of Science, Rehovot 76100, Israel

[7]Gastroenterology Unit, Rambam Health Care Campus, Bruce Rappaport faculty of Medicine, Technion, Haifa, Israel

[8]These authors contributed equally

[9]These authors contributed equally

[10]Senior authors

*Correspondence: Jacob H. Hanna (jacob.hanna@weizmann.ac.il); Alejandro Aguilera-Castrejon (alejandroac@weizmann.ac.il); Shadi Tarazi (shadi.tarazi@weizmann.ac.il); Itay Maza (i_maza@rambam.health.gov.il); Noa Novershtern (noa.novershtern@weizmann.ac.il)

@Lead Contact

Summary

In vitro cultured stem cells with distinct developmental capacities can contribute to embryonic or extra-embryonic tissues after microinjection into pre-implantation mammalian embryos. However, whether cultured stem cells can independently give rise to entire gastrulating embryo-like structures with embryonic and extra-embryonic compartments, remains unknown. Here we adapt a recently established platform for prolonged ex utero growth of natural embryos, to generate mouse post-gastrulation synthetic whole embryo models (sEmbryos), with both embryonic and extra-embryonic compartments, starting solely from naïve ESCs. This was achieved by co-aggregating non-transduced ESCs, with naïve ESCs transiently expressing Cdx2- and Gata4- to promote their priming towards trophectoderm and primitive endoderm lineages, respectively. sEmbryos adequately accomplish gastrulation, advance through key developmental milestones, and develop organ progenitors within complex extra-embryonic compartments similar to E8.5 stage mouse embryos. Our findings highlight the plastic potential of naïve pluripotent cells to self-organize and functionally reconstitute and model the entire mammalian embryo beyond gastrulation.

Introduction

Different types of stem cells can be grown in vitro and when injected into mouse pre-implantation embryos, they can contribute to embryonic or extraembryonic tissues. Mouse embryonic stem cells (ESCs) cultured in naïve conditions, can generate chimeric embryos following blastocyst microinjection, proving that these cells have the potential to make all tissues of the embryo proper (Bradley et al. 1996). Mouse embryo derived trophoblast stem cells (eTSCs) can be derived from early embryos (E3.5-E6.5) and can contribute to embryonic placenta (Tanaka et al., 1998).

Recent studies have been increasingly underscoring the ability of ESCs to be coaxed to self-assemble into complex structures in vitro such as blastoids, organoids, assembloids and gastruloids (Lancaster et al., 2013; Veenvliet et al., 2020), which open pathways for modelling developmental questions. For example, combining mouse ESCs with eTSCs, leads to blastocyst like structure formation, termed blastoids. However, the latter entities are not able to form embryos upon in utero transfer (Rivron et al., 2018). Gastruloids are small aggregates made from mouse ESCs that can recapitulate symmetry breaking and axis formation (Beccari et al., 2018). However, gastruloids do not exhibit primitive streak formation, and therefore do not model authentic gastrulation and cannot complete the gastrulation process either. Further, they can mostly mimic mid-posterior, rather than anterior, brain development and lack extra-embryonic compartments.

An alternative approach is the formation of embryoid models which are formed by aggregation of different types of embryonic and extra-embryonic stem cells (Harrison et al., 2017). Aggregating mouse embryo derived trophoblast stem cells (eTSCs), extraembryonic endoderm (XEN) (Kunath et al., 2005) cells with ESCs, leads to the formation of embryo-like structures resembling early ~E6.0 post-implantation embryos (Sozen et al., 2018). Early-gastrulation ~E6.5 stages can be reached when using Gata4 inducible ESCs instead of XEN cells (Amadei et al., 2021). However, it has not been possible to test and optimize developmental potential of such entities further, since transferring embryos at the post-implantation stage back into host uterus is not technically feasible even for natural embryos, and conducive platforms for ex utero embryogenesis from such embryonic stages were not available until recently, even for natural embryos (Aguilera-Castrejon et al., 2021). The proof of concept of whether and which in vitro cultured stem cells can generate whole embryo-like entities, with embryonic and extraembryonic compartments and that can proceed through gastrulation and initiate organogenesis, remains to be established.

Seeking to tackle this challenge was motivated by our recent ability to devise static and dynamic culture platforms and growth conditions that allow continuous capturing of natural mouse embryogenesis

from pre-gastrulation until late organogenesis stages ex utero (Aguilera-Castrejon et al., 2021). This was achieved by integrating roller culture system on a drum (New, 1978; Tam, 1998) with an in house developed electronic gas-and pressure regulation module (Aguilera-Castrejon et al., 2021). Moreover, we defined growth conditions (termed EUCM) that are optimal for growing post-implantation mouse embryos (Aguilera-Castrejon et al., 2021). This work established in a mammalian species, that the processes of gastrulation and organogenesis can be jointly and continuously recapitulated adequately in the petri dish, further motivating us to ask whether reconstituting these processes can be done ab initio from in vitro cultured stem cells upon being placed in these artificial ex utero experimental settings. We term such putative advanced post-gastrulation embryo-like models as synthetic Embryos (sEmbryos) or Synthetic Whole EMbryoids (SWEMs).

Results

Egg-cylinder shaped sEmbryos generated solely from naïve ESCs

Recent literature indicates that the naïve state of pluripotency can be coaxed to give rise to Trophoblast stem cells (TSC) and Primitive endoderm (PrE) lineages (Anderson et al., 2017; Blij et al., 2015). Mouse ESCs grown in naive 2i/Lif contribute at very low efficiency to extraembryonic placenta and yolk-sac (Morgani et al., 2013). Human naïve pluripotent cells can be coaxed to give rise to early progenitors of PrE cells and TSCs, even without the need for ectopic transcription factor overexpression (Bayerl et al., 2021). This suggests that the naïve pluripotent cells may theoretically serve as the entire source of embryonic and extra-embryonic tissues, and thus may enable the generation of entire advanced synthetic embryos by only starting with in vitro grown naïve ESCs, which remains to be experimentally shown.

Overexpression of Cdx2, a master regulator of TSC lineage, can lead to formation of mouse TSC lines (Niwa et al., 2005). Gata4 overexpression induces PrE lineage in ESCs (Fujikura et al., 2002) and early stage stem cell-derived embryoids (Amadei et al., 2021). Currently, all pre-gastrulation embryo-like models described were generated by using embryo derived TSC lines (eTSC) (Amadei et al., 2021). Therefore, we aimed to generate mouse synthetic embryos solely by aggregating naïve ESCs that transiently overexpress master regulatory transcription factors for both TSC and PrE lineages. We aimed to optimize conditions for rapid and efficient induction of TSCs from naïve ESCs (**Fig. 1A**). We generated Cdx2 Doxycycline (DOX) inducible ESCs (iCdx2) (**Fig. S1A**), that were subjected to another targeting to introduce an Elf5-YFP reporter (Benchetrit et al., 2019), which is a reliable marker for TSCs. After Cdx2 induction in TSCm conditions, Elf5 reactivation was evident at 72 hours (**Fig. 1B**). After 7 days of DOX induction, only ~30% of the cells expressed Elf5-YFP reporter (**Fig. 1B**). Nuclear YAP localization,

following Hippo signaling inhibition, in the early embryo (Kagawa et al., 2022), is a determinant for TE fate induction alongside Cdx2 expression. Thus, we tested TSC induction in iCdx2 cells with the addition of LPA, a Hippo pathway inhibitor. While 72h of DOX-LPA treatment was still the minimal time to see reactivation of endogenous Cdx2 allele expression (**Fig. S1C**), FACS analysis showed an acceleration in the efficiency in TSC induction in which up to ~75% of the population adopt TSC identity within 7 days (**Fig. 1B**) and even if DOX is stopped at day 3 (**Fig. S1D**). Further, naïve ESCs grown in 2i/Lif conditions yielded Elf5+ TSCs at ~14 fold higher efficiency than isogenic ESCs grown in serum/Lif conditions, and isogenic primed EpiSCs failed to generate mouse TSCs (**Fig. S1F-G**), consistent with previous results (Blij et al., 2015). Therefore, we focused on using mouse naïve ESCs grown in 2i/LIF conditions (Hanna et al., 2009; Nichols and Smith, 2009).

Kinetics of TSC induction from naïve ESC was evaluated by RNA-seq (**Fig. 1C**). Following 96h of Cdx2-LPA induction bulk cultures showed gene expression profiles that clustered together with established eTSC lines, while without LPA treatment, Cdx2 induction requires 3 passages (~13 days) to cluster with eTSC lines (**Fig. 1C, S1B).** We generated KH2-Gata4 mouse ES lines that overexpress Gata4 following DOX induction (iGata4 ESCs)**.** Like previous results (Amadei et al., 2021), endogenous expression of Gata4 and PrE markers can be detected at 24h post-induction, supporting priming of naïve PSCs towards PrE identity (**Fig. S1H-I**). PrE marker induction was absent when starting from isogenic iGata4 cells grown in primed EpiSC conditions (**Fig. S1J**).

We tested whether assembling the three naïve ESCs lines: WT, iGata4 and iCdx2 following DOX pre-treatment and co-aggregation up to day 5, can result in egg-cylinder like structures in vitro, and whether the cells segregate based on their transgenic priming (**Fig. 1D**). Each of the lines was transduced with a lentivirus constitutively expressing a different fluorescent label (**Fig. 1E**). iCdx2-mCherry lines correctly localized to the extraembryonic ectoderm (ExE) compartment in egg-cylinder shaped embryos (**Fig. 1F-H**). WT-BFP labeled ESCs predominantly contributed to the embryo proper, and iGata4-GFP labeled cells localized to the visceral endoderm (VE) surrounding the sEmbryos (**Fig. 1F-H**). Immunostaining for Oct4 (Epiblast), Tfap2c (ExE) and Sox17 (VE) at day 4 corroborated proper expression of linage markers by each donor cell population (**Fig. 1H**). Correct segregation and localization of each cell type was observed in approximately 25% of the sEmbryos (**Fig. 1G**). Failure of achieving proper segregation resulted from disproportionate and aberrant co-assembly between the three cell types following initial aggregation (**Fig. S2A**).

sEmbryos self-assembled from naïve ESCs develop ex utero up to early organogenesis

We examined the ability to generate egg cylinder shaped sEmbryos capable of reaching advanced post-gastrulation stages, made solely from starting populations of naïve ESCs, and then subdivided into three fractions based on short pre-treatment prior to their co-aggregation: (1) naive iCdx2 cells following DOX+/-LPA treatment in TSCm (which preferentially give rise to TSC lineage – **Fig. 1H**), (2) naïve iGata4 ESCs following 24h pre-treatment with DOX in 2i/Lif conditions (which preferentially generates PrE), and (3) naïve ESCs cultured in 2i/Lif conditions (**Fig. 2A**).

Optimizations were conducted to determine the DOX pretreatment regimen compatible with a relatively more productive outcome, and to define optimal cell numbers and ratios (**Fig. S2C-E**). The following conditions were found optimal (**Fig. 2A**): Gata4 pre-induction for 24h in 2i/Lif (or Aggregation Media (**AM**)) conditions; pre-induction of Cdx2 for between 24 hours up to 14 days in TSCm-LPA conditions prior to co-aggregation; and inclusion of DOX in Aggregation Media for the first 48 hours after aggregation. At day 3, AM was replaced by an optimized media termed Ex Utero Culture Media 2 (**EUCM2**). Due to their increase in size, the aggregates were combined and gently transferred to non-adherent tissue culture plates on a shaker placed inside a conventional tissue culture incubator in EUCM2 which improved the outcome (**Fig. S3, S2E**). At day 5, egg-cylinder shaped sEmbryos (**Fig. 2B**) were manually picked and transferred to the ex utero roller culture system in previously established Ex Utero Culture Medium (EUCM) conditions (**Fig. 2C, S3**), that were originally developed to support natural embryos growth from E5.5 until E11 (Aguilera-Castrejon et al., 2021). From day 5 to day 8, sEmbryos continued to be grown in the roller culture system (**Fig. S3, Supplementary Video S1-S5**). Consistent with TSC induction ability in naïve ESCs by Cdx2 overexpression alone (**Fig. 1B**), Day 8 sEmbryos can be obtained without the use of LPA in the pre-induction phase of iCdx2, albeit with much lower efficiency. Continuing only with the static conditions in days 5-8 yielded a detrimental outcome **(Fig. 2G and S2E).**

This 8-day protocol supported the self-organization and growth of naïve ESC derived aggregates into organogenesis stage sEmbryos that grow within extraembryonic membranes (**Fig. 2D-F**), comparable to E8.5 in utero developed natural embryos. Adequately developed day 8 sEmbryos did not show further advance in development upon additional culture for one more day and suffered from aberrantly enlarged heart with profound pericardial effusion at day 9 (**Fig. S2B**). Synthetic entities grown from day 4-7 in previously published static and IVC medium based protocols (that involve the use of knockout serum replacement - KSR), did not develop further than previously achieved (Amadei et al., 2021) and yielded empty yolk sacs (**Fig. 2G, S2E**).

sEmbryos recapitulate morphological changes occurring during natural embryo development

sEmbryos originating from naïve ESCs starting populations faithfully resembled all stages of natural post-implantation development (van Maele-Fabry et al., 1992; Parameswaran and Tam, 1995; Tam and Snow, 1980), going through luminogenesis, symmetry breaking and gastrulation, until early organ formation (**Fig. 2B**). Egg cylinder shape sEmbryos start emerging on day 3 of the protocol**,** when aggregates start luminogenesis and an outer cell layer is formed, and without going through a blastocyst-like morphology in the earlier days. At day 4, the aggregates show similar morphology to an E5.5 embryo, with clear segregation into the epiblast (Epi) and extra-embryonic ectoderm (ExE) compartments surrounded by a layer of visceral endoderm (VE) cells (**Fig. 2B**). At day 5, sEmbryos closely resemble E6.5 embryos, showing a clear difference between the cup-shaped epiblast and the ExE, both enveloped by the VE **(Fig. 2B)**. The Epi displays an expanded pro-amniotic cavity (PAC), and successfully break symmetry showing an incipient primitive streak in one side of the epiblast, adjacent to the ExE (**Fig. 2B**). After 6 days the sEmbryos reach the neural plate stage. The amniotic folds fuse to form the amnion (Am), generating the amniotic (AC) and exocoelomic cavities (EC) (**Fig. 2B**), and an incipient allantoic bud (AB) is observed in the ExE compartment at the opposite side of the neural plate.

At day 7 there is a major expansion of the yolk sac (YS), which by then surrounds the embryo, mimicking what happens in natural embryos; while in the Epi compartment the anterior ectoderm begins to form a broad plate, the future neural groove, making evident the emergence of the head-to-tail axis (**Fig. 2B**). In the ventral part of sEmbryos at day 7, the migration of the primitive streak and the heart field are evident, and the foregut invagination starts to be seen, like E8.0 natural embryos (**Fig. 2B**). At day 8 the sEmbryos resemble the morphology of E8.5 embryos (**Fig. 2E-F**). The dorso-ventral axis of sEmbryos is clearly seen by the neural folds facing the amnion dorsally opposite to the foregut facing the yolk sac ventrally (**Fig. 2E-F**) (**Supplementary Video S2**). The sEmbryos continue growing completely enveloped inside the extra-embryonic membranes (yolk sac and amnion) and present an ectoplacental cone (EPC) structure in the opposite side of the embryo (**Fig. 2E**). The blood islands (BI) are visible in the lateral sides of the yolk sac (**Fig. 2E**), and blood begins to circulate in the yolk sac vessels (vitelline circulation). The sEmbryos display well-formed head folds, neural tube, invaginating foregut, beating heart, and up to 4 pairs of somites, followed by the tail (**Fig. 2F**), demonstrating the complete establishment of the head-to-tail and dorso-ventral axis (**Supplementary Video S2**). The allantois extends from the posterior part of the sEmbryo, connecting the tail to the EPC (**Fig. 2E**).

Of the normally egg cylinder-shaped embryos at day 5 (**Fig. 1G**) chosen for further growth in the roller ex utero culture until day 8, ~2% develop into sEmbryos comparable to E8.5 natural ones (**Fig. S5B-C**), yielding an effective 0.1%-0.5% normal day 8 sEmbryo development efficiency from total initial aggregates generated (**Fig. S5D-E)**. Although there is variation in size among adequately developed sEmbryos at Day 8, they were comparable to in utero developed natural E8.5 embryos (**Figure S4C**). Abnormal day 8 obtained sEmbryos can display a variety of abnormalities at the anterior, mid, or posterior regions, such as lack of neural folds or other body segments, as well as neural fold fusion, or development outside the yolk sac, which is not correlated to their size **(Fig. S4C-D)**.

Adequate spatiotemporal expression of lineage markers in advanced sEmbryos

We confirmed proper expression of canonical markers for the three cell lineages expected to be present in the mouse embryo at the egg cylinder-stage: a cup-shaped Epiblast positive for Oct4 and Otx2, the extra-embryonic ectoderm (ExE) adjacent to the epiblast expressing Cdx2, Tfap2c and Eomes, and the visceral endoderm (VE) positive for Gata4, Gata6, Sox17 and Foxa2 enveloping both compartments (**Fig. 3, S4A-B**). Otx2 and Eomes were present also in the embryonic VE (**Fig. 3A, S4A-B**). Sox2 expression in the Epi compartment as well as the ExE was correctly recapitulated in sEmbryos. Further, proper establishment and migration of the AVE from the distal part of the epiblast towards the future anterior part was evidenced by the staining for BMP antagonist Cer1 at day 4, either at the distal tip of the epiblast or asymmetrically located towards one side of the egg cylinder (**Fig. 3B**).

On day 5, a population of Brachyury^{+} cells appeared at the posterior side of the epiblast near the ExE boundary, opposite to Cer1 and Dkk1, corroborating the appearance of the primitive streak and the onset of gastrulation in day 5 sEmbryos (**Fig. 3C**, **S4B**). At day 6, the population of Brachyury^{+} cells expanded and migrated towards the distal part of the Epi, between the VE and the Epiblast (**Fig. 3E**). Among the egg-cylinder shaped sEmbryos at day 6, 38% exhibit clear antero-posterior asymmetry, evidenced by formation of the neural plate in one side of the epiblast (**Fig. 3D**). Emergence of the axial mesoderm was evident by the presence of Foxa2/Brachyury^{+} cells at the distal tip of the primitive streak, as described for natural embryos at E7.5 (**Fig. 3E**). We identified definitive endoderm cells in sEmbryos at day 6 by co-staining of Sox17/Foxa2, while a population of Foxa2+/Sox17- cells allocated along the distal tip of the egg-cylinder identifies the emerging midline of the embryo (**Fig. 3F**).

To analyze the emergence of primordial germ cells (PGCs) in sEmbryos we employed the Blimp1-mVenus Stella-CFP reporter found in the BVSC ESC line (Hayashi et al., 2011). We detected activation of the Blimp1-mVenus fluorescent reporter at day 5, specifically at the site of putative the primitive streak, in

the boundaries of the Epi/ExE (**Fig. 3G – upper row**). FACS analysis confirmed the emergence of PGC population in day 5 sEmbryos which is known to originate first as Blimp1+Stella- cells in the developmentally equivalent natural E6.5 embryos (**Fig. 3H**). We observed migration of PGCs in sEmbryos to the posterior ventral part of the embryos at day 8 by Sox2 immunostaining (**Fig. 3G – lower row**).

In addition to the morphological similarities observed between day 8 sEmbryos and E8.5 natural embryos (**Fig. 2B. S5A),** we corroborated proper differentiation and tissue morphogenesis by assessing the expression of several lineage-specific markers by whole-mount immunofluorescence. The neural folds (NF) and neural tube (NT) derived from the epiblast ectoderm, presented strong Sox2 expression, properly allocated along the antero-posterior axis of the sEmbryo, while Brachyury+ cells were found along the embryonic midline, resembling the elongated notochord (Nc) and tail bud (**Fig. 4A**). Otx2 marks the embryonic forebrain and midbrain in the natural E8.5 embryo and was detected in the anterior part of the neural folds in sEmbryos (**Fig. 4A, S5F**), while the neural-specific marker Pax6 was expressed in forebrain, hindbrain and neural tube of the sEmbryos, colocalizing at the forebrain region with Otx2, which mimics the pattern observed in natural embryos (**Fig. 4A)**. Foxa2, which is restricted to the notochord floor plate at the midline of the E8.5 embryo, was also detected in day 8 sEmbryos (**Fig. S5F**). The cardiac marker Myosin Heavy Chain II (MHC-II) was visible at the anterior ventral part of the sEmbryo, specifically localized in the heart bud (**Fig. 4A, S5G**), colocalizing with Gata4 which is also observed at the caudal end of the heart, definitive endoderm and the yolk sac. The Hox gene Hoxb4, expressed at the anterior-most somitic and paraxial mesoderm as well as at the caudal hindbrain, corroborated the formation of pairs of somites adjacent to the neural tube in iCdx2 sEmbryos (**Fig. 4B**). The expression patterns of Sox17, which labels endoderm-derived tissues at the gut tube area and the yolk sac, and Sox9 which identifies the neural crest and notochord (Sox9) were also properly allocated in day 8 sEmbryos (**Fig. S5F)**.

To further analyze the extent of tissue patterning in sEmbryos, we performed transversal plane cross-sectioning at the anterior, mid and caudal regions of day 8 sEmbryos, particularly of the embryonic neural tube and heart (**Fig. 4C**). Sox1 and Foxa2 co-staining indicated proper establishment of the dorso-ventral axis in the neural tube, evidenced by the double positive cells specifically located at the ventral part, resembling the floor plate in natural embryos (**Fig. 4D**). Folding and complete closure of the proximal region of the neural tube was observed in day 8 sEmbryos, which corresponds to what has been described in natural embryos (**Fig. 4D**). Histological examination of the entire body of the sEmbryos revealed high similarities at the tissue-level between iCdx2 sEmbryos and E8.5 in utero control, both at the anterior and the posterior parts of the embryos **(Fig. 4E, S5H)**.

At E8.5, the primitive heart tube undergoes looping and develops into a chambered heart (Mandrycky et al., 2020). We observed the emergence of functional beating heart, that in turn propels blood circulation in the sEmbryos at day 8 (**Supplementary Video S2**). Histological examination of the developing heart demonstrated similar morphology to the E8.5 natural embryo, showing formation of the heart chambers and development of the myocardium and the endocardium lining the inner side of the heart (**Fig. 4E-F**), suggesting proper recapitulation of heart morphogenesis. We further analyzed heart differentiation and patterning different markers of the developing heart (Gata4, Gata6, Nkx2.5 and MHC-II), all of them showing proper expression in the heart tube of the sEmbryos (**Fig. 4F**).

Embryo derived TSC lines can propel self-organization in advanced sEmbryos

We next proceeded to test whether embryo-derived TSC lines (eTSC) (Tanaka et al., 1998) can functionally generate post-gastrulation synthetic embryos that have also initiated organogenesis, which has not been achieved so far. We co-aggregated WT naïve ESCs together with Dox-treated iGata4 ESCs and eTSC to generate synthetic embryos (**Fig. 5A**). The cells self-organized into egg-cylinder stage embryos resembling the E5.5 post-implanted natural embryo after 4 days (**Fig. 5B**). On Day 5, sEmbryos displayed antero-posterior asymmetry and began gastrulation as evidenced by the PS marker Brachyury (**Fig. 5B-D**), as it occurs in E6.5 natural embryos and iCdx2 sEmbryos. Six days after aggregation, the PS extends to the distal tip of the epiblast, the amniotic fold extends reaching the anterior part of the egg-cylinder, the allantoic bud is specified and axial mesoderm (Foxa2/Brachyury double positive cells) emerge in the PS (**Fig. 5B, D)**. This stage represents the current limit reported in former studies (Amadei et al., 2021). By means of live imaging and flow cytometry, we confirmed the appearance of Blimp1^{+} PGCs at day 5 and Stella^{+} PGCs in day 6 sEmbryos (eTSC) (**Fig. 5E**). Properly developed egg cylinder-sEmbryos day 5 were chosen for further ex utero culture in EUCM. Day 8 sEmbryos generated with eTSC developed until organogenesis stages surrounded by the extraembryonic membranes and were morphologically comparable to E8.5 natural embryos developed in utero (**Fig. 5B**). Immunostaining analysis for germ-layer markers showed a similar patterning to natural stage-matched embryos (**Fig. 5F**) and day 8 iCdx2 sEmbryos (**Figure 4**). Day 8 sEmbryo derivation efficiency was four fold higher when using eTSC than iCdx2 approach (**Fig. S5E**).

Development of extraembryonic compartments in post-gastrulation sEmbryos

We sought to further characterize the extraembryonic tissues in sEmbryos. At day 7, the yolk sac starts to enlarge and engulf the embryo dorsally. The amnion, ectoplacental cone, and yolk sac blood islands become evident (**Fig. 6A, Supplementary Video S2**). At day 8, the sEmbryo develops completely within the yolk sac and amnion, with the amnion being the innermost membrane enveloping the embryo-

proper from the dorsal part, surrounded by the vascularized yolk sac with the ectoplacental cone attached to it on the opposite side of the sEmbryo (**Fig. 6A-B**). Moreover, the presence and expression pattern of Foxa2 and Sox17 in yolk sacs and ectoplacental cones of day 8 sEmbryos (both iCdx2 and eTSC based ones), closely resembles that of natural in utero E8.5 embryonic extraembryonic compartment (**Fig. 6C**).

Blood islands were widely visible and abundant in developing synthetic yolk sacs (**Supplementary Video S2**), and immunostaining of whole yolk-sacs for Runx1 which marks these primitive hematopoietic progenitors, termed erythromyeloid progenitors (EMPs) confirmed their identity (**Fig. 6D**). FACS analysis confirmed authentic expression of defining surface markers delineating the different subpopulations within the hematopoietic progenitors in the embryonic yolk sac compartment in sEmbryos, as previously described in natural embryos (Iturri et al., 2021) (**Fig. 6E**). We applied a functional erythroid specific methylcellulose-based assay to validate erythroid colony formation and expansion potential. sEmbryos derived blood progenitors formed typical erythrocyte colonies with appropriate morphology (**Fig. 6F**).

scRNA-seq analysis validates mouse sEmbryo complexity

To characterize and annotate the various cell types present in the advanced synthetic embryos generated herein (iCdx2 or eTSC based) in a more quantitative and unbiased manner, we performed single cell RNA-sequencing (scRNA-seq) (**Fig. S6A**). A total of 40,657 cells were collected from Day 8 sEmbryos with ~E8.5 like morphology: 3 sEmbryos that were developed from iCdx2 cells following brief 3 day DOX based induction (Day -1 until day +1), 4 sEmbryos that were developed following iCdx2 cells following 10 day DOX based induction (Day -8 until day +1), and 2 sEmbryos that were developed from eTSC cells (**Fig. 7A-B**). In addition, a total of 26,948 cells were collected from natural in utero grown E8.5 embryos that serve as a reference control.

Clustering analysis based on differentially expressed genes revealed 23 different cell states **(Fig. S6B, Fig. 7A)**. Subsequently, the identity of the clusters was annotated based on specific marker genes of the major cell lineages previously defined by single-cell transcriptomics of early mouse embryos (**Fig. S6B-C**) (Ibarra-Soria et al., 2018). All three germ layers were represented, as well as all extraembryonic tissues, in one or more clusters, indicating the presence of different cell states within those lineages in a similar manner in both in utero grown natural embryos and ex utero grown sEmbryos (**Fig. 7A, C**). When examining sEmbryo biological replicates either from iCdx2 or eTSC based protocols, or when examining a single embryo based single cell RNA-seq sample (short iCdx2 induction), similar results were obtained (**Figure 7B**). Such high overlap was not observed when comparing to E6.5 or E10.5 natural embryos (**Fig. S6D**).

The profile of cell types found in day 8 sEmbryos developing ex utero was highly similar to E8.5 natural embryos, demonstrating that lineage differentiation complexity and commitment are faithfully recapitulated in synthetic embryos at the single cell level (**Figure 7B-C**). This analysis confirmed that the composition of cell transcriptional states in the sEmbryos developing ex utero until early organogenesis is equivalent to their natural counterparts. Comparison of the relative cell proportions of different cell types in sEmbryos and natural embryos showed no significant differences in the majority of clusters, while some differences were found in only six of the cell clusters (**Figure 7D**). These selective differences in certain population abundance were not similar to minor differences seen in abundance when comparing day 8 sEmbryo to ex utero grown E8.5 natural embryos (**Figure S6E-F**), suggesting that these differences are not a result of the ex utero growth platforms per se, but rather result from the synthetic origin of the day 8 sEmbryos analyzed.

Transcriptionally, 22 of the 23 cell clusters showed very high correlation (0.93-0.98) in day 8 sEmbryos when compared to E8.5 natural embryos (**Fig. S7A**). Specific markers for tissues such as somitic mesoderm, notochord, neural tube, and cardiac tissue were expressed specifically in their corresponding tissue cluster, both in sEmbryos and in natural embryos (**Fig. S7B**). Similar conclusions could be reached when focusing on specific markers (Mittenzweig et al., 2021) for different extra-embryonic tissues (**Fig. S7B**). Examining the expression of key placental markers and comparing between day 8 synthetic embryos to E8.5 natural ex utero and E8.5 natural in utero grown embryos, shows that while most markers are expressed in all three groups, some trophoblast giant cell and spongiotrophoblast markers (Lee et al., 2016) were absent or nearly-absent in both natural and synthetic ex utero grown embryos, suggesting that this is predominantly a result from the absence of a maternal-fetal interface in protocols entailing ex utero embryogenesis (**Fig. S7C**). Overall, these results prove that despite of differences and abnormalities noted above, day 8 synthetic embryos are remarkably similar to their natural E8.5 counterparts grown either in utero or ex utero.

Discussion

We report that our recently developed electronically controlled ex utero embryo culture platform and conditions, that enable faithful and continuous capturing mouse natural gastrulation and organogenesis ex utero (Aguilera-Castrejon et al., 2021), can also support ex utero self-organization of post-gastrulation synthetic embryos that are generated by co-aggregating stem cells. The aggregated naïve pluripotent stem cells assemble, while undergoing lineage priming, into egg-cylinder shaped and then into complete embryo-like models that accomplish gastrulation and proceed significantly beyond to develop brain (including fore-

mid brain regions), neural folds, neural tube, gut tube, beating heart, somites, and progenitors of other organs. The sEmbryos described herein develop within extraembryonic membranes as natural embryos, and without the need to provide external targeted signaling pathway induction. This study underscores the dormant self-organization capability of naïve pluripotent stem cells into advanced organized whole embryo-like entities ex utero.

Our findings establish that the trophoblast derived extraembryonic compartment in advanced sEmbryos can be generated solely from mouse naïve pluripotent stem cells and need not be only obtained from natural embryo derived TSC lines. The latter demonstration is important given previous reports indicating that mouse ES derived TSCs do not complete their transition to authentically adopt eTSC identity (Cambuli et al., 2014). It is possible that the use of Hippo pathway inhibitor in our protocol helped minimize these differences. Closer molecular and functional interrogation of different TSC growth conditions and heterogeneity among TSCs (Seong et al., 2022) is of future scientific interest.

The generation of post-gastrulation mouse synthetic embryos and only by starting with naïve ESCs, could expand the experimental platforms available to interrogate early embryonic developmental biology from multiple species. Building on the knowledge, logic and devices to expand advanced complete mouse synthetic embryo models as described herein, together with harnessing recent advances in human naïve pluripotency growth conditions (Gafni et al., 2013; Bayerl et al., 2021), researchers may become closer to generate human synthetic embryoid models ex utero, and solely from human naïve iPSCs. Although, as shown herein, synthetic whole embryoids are not identical to embryos, they may still be utilized in the future as an invaluable model for inaccessible time windows during early developmental embryology research and modelling human developmental malformations. The latter may also constitute a platform for inducing progenitor populations from human naive iPSCs by tapping on the self-organization capacity of naïve iPSCs into synthetic whole embryoid models (SWEMs) under optimized ex utero growth platforms and conditions. Cells and tissues from such synthetic advanced organized entities, could be potentially useful for cell differentiation research and transplantation biotechnology.

Limitations of the study

Naïve pluripotent stem cell growth conditions that utilize FGF/MEK signaling inhibition, cause loss of imprinting, which perturbs the developmental potential of such cells (Choi et al., 2017). This risk may possibly be mitigated in the future by using naïve conditions with titrating down the concentration of inhibitors or alternative naïve conditions (Bayerl et al., 2021; Shimizu et al., 2012). We note that eTSC

lines show reduced yield in synthetic embryo formation following prolonged passaging, consistent with reduction in Elf5+ cell fraction upon extended passaging (**Fig. S1E**). The latter may be resolved by inducing naïve ESCs towards becoming TSCs which can be transiently induced during each aggregation experiment.

The reduced efficiency and heterogeneity observed during the formation of synthetic embryos can be a complicating factor. Furthermore, day 8 sEmbryo formation efficiency is variable between ESC lines used, with some ESC lines tested could not generate sEmbryos beyond day 6 of the protocol. It is plausible that upon further experimentation the efficiency and variability in synthetic embryo formation can be improved in the future. Further, the ex utero system and conditions utilized herein has been shown to be able to support the growth of natural embryos up to E11 (Aguilera-Castrejon et al., 2021), however sEmbryos described herein could only reach E8.5 so far. It remains to be known whether further improvements of the aggregation protocol or the ex utero growth platform can overcome this barrier. We cannot exclude that alternative ex utero culture platforms, aggregation strategies or growth conditions might yield similar or enhanced results relative to the ones reported herein.

Finally, while most synthetic embryos obtained show differences and abnormalities when stringently compared to natural embryos, the generation of integrated synthetic embryo models that adequately complete gastrulation and initiate neurulation and organogenesis within the synthetic extraembryonic tissues surrounding them, will likely be very useful as they can still be used to evaluate in vitro stem cell differentiation with greater complexity relative to any other currently available stem cell derived in vitro models.

Acknowledgments: This work was funded by Pascal and Ilana Mantoux; Flight Attendant Medical Research Institute (FAMRI); MBZUAI-WIS Program, European Research Council; ISF; Minerva; Israel Cancer Research Fund (ICRF), Kimmel Stem Cell Research Center, and BSF.

Author contributions: S.T. and A.A.C. established sEmbryo ex utero culture, designed and conducted most of the wet lab work, sequencing, conducted embryo immunostaining and imaging, optimized Cdx2 pre-induction treatment and wrote the manuscript. S.T. generated cell lines with assistance from S.V and optimized the final sEmbryo culture protocol. C.J. conducted immunostaining experiments, confocal imaging and lentivirus labeling experiments. S.A. performed immunohistochemistry sections. F.R. and E.W. assisted in immunostainings and imaging. N.G. and I.M. recruited donors and performed umbilical cord blood and serum extraction. M.H. conducted yolk sac erythroid progenitor analyses under the supervision of T.L. E.G.C. assisted in immunostainings and embryo dissections. B.O. assisted in embryology analysis. S.V. generated plasmids. S.N.T, M.R, S.H., N.L. assisted in condition optimizations. C.R. and O.B. - histology. M.K. and H.K.S - RNA library preparation and sequencing. N.N. - bioinformatics analysis. J.H.H. and A.A.C conceived the idea for the project (with S.T.), supervised data analysis and manuscript writing.

Declaration of interests: J.H.H has submitted patent applications relevant to the findings reported herein and is a chief scientific officer of Renewal Bio Ltd. that has licensed technologies described herein.

Inclusion and Diversity: One or more of the authors of this paper self-identifies as an underrepresented ethnic minority in science. One or more of the authors of this paper self-identifies as a member of the LGBTQ+ community. One or more of the authors of this paper received support from a program designed to increase minority representation in science.

Figure Legends

Figure 1. Proper self-allocation of naïve ESC derived cells in sEmbryos following transient ectopic expression of Cdx2 and Gata4

A. Scheme demonstrating screening strategy for efficient TSC induction using iCdx2 Elf5-YFP reporter line. **B,** Fraction of Elf5 expressing cells measured by flow cytometry after different times of DOX mediated Cdx2 induction in TSC medium (TSCm) with or without 1μM LPA. **C,** Spearman correlation matrix between expression profiles of mouse embryonic fibroblasts (MEFs), naïve ESCs, XEN cells, embryo derived TSC lines (eTSC) and DOX induced Cdx2 ESCs under TSCm culture conditions at different time points (with or without LPA). **D,** Schematic of fluorescent labeling strategy of different naïve ESC line followed by co-aggregation and self-assembly of egg-cylinder shaped synthetic embryos (sEmbryos)**.** iGata4 and iCdx2 ESCs were exposed to DOX 24h before until 48h after co-aggregation. **E,** Microscope fluorescent imaging and flow cytometry of BFP, GFP and mCherry labeled ESCs. **F,** Live confocal imaging of egg-cylinder shaped sEmbryos after 3 to 5 days of aggregation. A random field is shown in the upper panel, and an image of a single sEmbryo with proper segregation is shown in the lower panel. **G,** Percentage of egg-cylinder shaped sEmbryos presenting proper segregation of lineages. Dots represent efficiency percentage in random fields of view; data are mean ± s.e.m. **H,** Middle-section immunostainings of day 4 sEmbryos stained for Epi (Oct4), ExE (Tfap2c) and VE (Sox17) markers.

Figure 2. Naïve ESC derived sEmbryos complete gastrulation and initiate neurulation and organogenesis stages within extraembryonic membranes

A, Schematic depiction of the sEmbryo generation and culture protocol. DOX Pre-induction (-1 day for Gata4 in 2i/Lif or AM, and -14 up to -1 days for Cdx2 in TSCm +/- LPA) and aggregation of 3 types of naïve ESCs derived populations followed by culture in AM (with DOX in first 2 days), EUCM2 and EUCM for 8 days generates self-organized sEmbryos (iCdx2) that grow up to early organogenesis. **B,** Bright field images of sEmbryos at each day of the culture protocol compared to stage-matched natural embryos where indicated. **C,** On Day 5 putative sEmbryos were transferred into electronically controlled roller bottle ex utero culture platform set-up that was used for sEmbryo propagation until day 8. **D,** View of day 7 and day 8 sEmbryos cultured ex utero inside the roller culture bottles. **E,** Bright-field images of day 8 sEmbryos growing ex utero within whole extraembryonic membranes (yolk sac and amnion). **F**, Day 8 sEmbryo (iCdx2) and E8.5 natural embryos after dissection and removal of extraembryonic membranes. Insets are enlargements of the dashed boxes. **G,** Image of empty yolk sacs obtained after continuous culture in IVC media (with KSR) and static culture-based protocol. A; anterior, AC, amniotic cavity; Am, amnion; Al, allantois; AB, allantoic bud; BI, blood islands; EC, exocoelomic cavity; Epi, epiblast; EPC, ectoplacental cone; ExE, extraembryonic ectoderm; Fg, foregut pocket; H, heart; NF, neural folds; NT, neural tube; OP,

Optic pit; P, posterior; PAC, pro-amniotic cavity; PS, primitive streak; S, somites; TB, tail bud; VE, visceral endoderm; YS, yolk sac.

Figure 3. Expression patterns of lineage markers in egg-cylinder shaped sEmbryos (iCdx2) resemble those of natural embryos

A, Middle section confocal images of day 4 egg cylinder sEmbryos and natural E5.5 embryos immunostained for ExE, VE and Epi markers. **B,** Migration of the AVE from the distal to the future anterior part revealed by Cer1 staining (magenta) in day 4 sEmbryo. **C,** Immunofluorescence images (middle section) of VE, trophoblast, epiblast and gastrulation markers (Brachyury, yellow arrows) in day 5 sEmbryos compared to matched E6.5 natural embryos. **D,** Quantification of antero-posterior asymmetry in sEmbryos at day 6 as measured by presence of the anterior neural plate. Dots represent percentage of embryos showing evident anterior neural plate per field of view; data are mean ± s.e.m. of 4 different experiments; n = 22 fields of view evaluated. **E-F,** Migration of the primitive streak and establishment of the definitive endoderm in sEmbryos at day 6 and control E7.5 natural embryos. **E,** Immunofluorescence images showing migration of Brachyury^{+} cells and presence of Brachyury/Foxa2 double positive cells. **F,** Sox17/Foxa2 immunostaining exposing invaginating definitive endoderm cells; Foxa2/Sox17 cells along the epiblast reveal the embryonic midline in sEmbryos. Insets are enlargements of the dashed boxes. **G,** Middle section images of Blimp1-mVenus fluorescence at day 5 sEmbryos detected by live imaging marking PGC specification (upper panel). Sox2^{+} PGCs show proper allocation to the anterior ventral side of the sEmbryos (iCdx2) at day 8 (lower panel). **H,** Flow cytometry plots for Blimp1-mVenus/Stella-CFP in dissected posterior epiblast of sEmbryos (iCdx2) at day 4 and day 5, marking their emergence at day 5 (equivalent to E6.5).

Figure 4. Day 8 post-gastrulation sEmbryos (iCdx2) properly recapitulate spatial expression patterns of tissues derived from all three germ-layers

A, Whole-mount immunofluorescence images of day 8 sEmbryos (iCdx2) showing proper expression of ectodermal (Sox2, Otx2, Pax6), mesodermal (MHC-II, Brachyury) and endodermal (Gata4) lineage markers, compared to natural in utero E8.5 embryos. **B,** Maximum intensity projection confocal images of Sox2 and Hoxb4 immunostainings highlighting the presence of somites (yellow arrows). **C**, Schematic representation of the cutting planes for transversal sections of the anterior- and mid-neural tube shown in **D** and **E**. **D,** Immunostaining (mid-section, transversal plane) of the closed neural tube in day 8 sEmbryos (iCdx2) compared to natural in utero E8.5 embryos. **E,** H&E staining of anterior and caudal transversal sections of day 8 sEmbryos and their natural counterparts at E8.5, displaying the embryonic neural tube, foregut pocket and heart (myocardium and endocardium) at the anterior region and gut lumen, neural tube

and tail neural groove at the posterior. **F,** Immunohistochemistry images (mid-section, transversal plane) of heart lineage markers in day 8 iCdx2 sEmbryos as compared to natural stage-matched embryos. A, anterior; D, dorsal; EC, endocardium; FB, forebrain; Fg, foregut pocket; H, heart; LV, left ventricle; MB, midbrain; MC, myocardium; Nc, notochord; NF, neural folds; NT, neural tube; P, posterior; RV, right ventricle; S, somite; TB, tail bud; TNG, tail neural groove; V, ventral.

Figure 5. eTSCs support development of advanced sEmbryos ex utero

A, Schematic of the sEmbryo (eTSC) generation and culture protocol. **B,** Bright-field images of sEmbryos (eTSC) developing ex utero from 0 to 8 days compared to equivalent natural in utero embryos. **C**. Middle-section immunofluorescence images of day 5 sEmbryos (eTSC) showing the correct localization of the Epi marker Oct4 and the primitive streak marker Brachyury compared to equivalent natural embryos. **D,** Primitive streak migration and invagination of endoderm in day 6 sEmbryos (eTSC) revealed by Brachyury (red) and Foxa2 (green) immunostainings. **E,** Live imaging of Blimp1-GFP sEmbryos exposing activation of the reporter in the PGCs at the posterior side of the embryo (upper panel) in day 5. Flow cytometry plots for Stella-mCherry single positive population in sEmbryos (eTSC) at Day 4 and dissected posterior epiblast of Day 6 sEmbryo (lower panel). **F,** Whole-mount immunostaining images of tissue-specific markers expressed in day 8 eTSC sEmbryos showing proper expression of ectodermal (Sox2, Otx2, Pax6), mesodermal (MHC-II, Brachyury) and endodermal (Gata4) lineage markers. A, anterior; AC, amniotic cavity; Am, amnion; Al, allantois; AB, allantoic bud; BI, blood islands; Epi, epiblast; EPC, ectoplacental cone; ExE, extraembryonic ectoderm; Fg, foregut pocket; H, heart; NF, neural folds; NT, neural tube; P, posterior; PAC, pro-amniotic cavity; PS, primitive streak; S, somites; VE, visceral endoderm; YS, yolk sac.

Figure 6. sEmbryos grow within extraembryonic membranes and develop allantois, blood islands and ectoplacental cone

A, Images of day 7 and day 8 sEmbryos showing the presence of amnion, yolk sac, allantois, ectoplacental cone, neural fold, head and blood islands. **B,** Schematic illustration of the extraembryonic compartments present in day 8 sEmbryos/E8.5 embryos. **C,** Whole-mount immunofluorescence images of markers present in yolk sacs isolated from sEmbryos at day 8 and E8.5 natural embryos. **D,** Runx1 immunostaining marking blood progenitors in yolk sacs. **E,** FACS contour plots for CD45 and CD34 expression among Lin^{-} $cKit^{+}$ $CD41^{+}$ progenitor cells. **F,** Methylcellulose in vitro culture of colony forming potential and morphology of erythroid progenitors derived from indicated samples.

Figure 7. scRNA-seq analysis of post-gastrulation mouse synthetic embryos

A, UMAP plot displaying individual cells. Points are colored according to their assigned cell cluster. Cell

lineage annotation of clusters based on marker genes of the major cell types identified in E8.5 mouse embryos. EN = total Embryo Number; CN = total Cell Number. **B**, UMAP plot displaying individual cells of the different samples as indicated. Colors as in (**A**). **C**, E8.5 natural embryo cells (black) and day 8 synthetic embryo cells (red) projected on the same UMAP plot. **D**, Pie charts depicting the proportional abundance of each cell cluster in both natural embryos and sEmbryos. Asterisks denote clusters with statistically significant differences between the two groups. * FDR corrected t-test $p<0.1$

Supplementary Figure Legends

Figure S1. Optimization of iCdx2 and iGata4 induction conditions (Related to Figure 1)

A, Bright field images of TSC derived from ectopic expression of Cdx2 in naïve ESCs over different indicated time points (upper panel), and immunostaining for TSCs markers Ap2y, Cdx2, Elf5 and Tbr2 along with pluripotency markers Nanog and Oct4 in iCdx2 ESC (clone #3) induced with DOX in TSC media (TSCm) for short term 72h or long-term passage 7 TSC line (lower panel). Scale bar, 50µM. **B,** RT-PCR analysis for TSC markers Hand1, Fgfr2, Elf5, Dppa1 and primitive endoderm markers Gata4, Gata6 and Pdgfra expression in iCdx2 clone #3 after DOX in TSC media supplemented with lysophosphatidic acid (LPA) 1µM. Analysis was done at different time points from 24h up to 120h. Values were normalized to Gapdh and compared to basal naïve state expression level. **C**, RT-PCR analysis for endogenous Cdx2 gene levels in iCdx2 clone 3 after treatment with DOX for different time points in TSC media supplemented with 1µM lysophosphatidic acid (LPA). Values were normalized to Gapdh and compared to basal naïve state expression level. **D**, Flow cytometry analysis presenting fraction of positive Elf5 population after treatment of iCdx2 with DOX in TSC media with 0.5 µM LPA for different time points up to 9 days, and fraction of positive Elf5 after short treatment with DOX for 3 days in TSC media with 0.5 µM LPA, then cultured the cell in TSC media with or without LPA for additional 3 days or 6 days. **E**, Flow cytometry analysis presenting fraction of positive Elf5 population after treatment of DOX and culture in TSC media for 6 passages and 9 passages. **F**, Fraction of positive Elf5 population after treatment of iCdx2 cells with DOX in TSCm for 3 days. Prior to DOX induction in TSCm, iCdx2 cells were cultured in primed Fgf/Activin, naïve Serum/Lif or naïve 2i/Lif condition for at least 3 passages. **G**, RT-PCR analysis for trophectoderm markers Cdx2, Hand1, Dppa1, Fgfr2 and Elf5 expression in iCdx2 clone cultured in primed or naïve conditions and induced with DOX for 72h in TSCm. **H**, RT-PCR analysis for primitive endoderm markers Foxa2, Pdgfra, Gata6, Hnf4a and Sox17 expression and TSC markers Gata3 and Gata2 expression in representative Gata4 clone after treatment with DOX in 2i/Lif media. Analysis done at different time points from 24h up to 96h. **I**, RT-PCR analysis for both endogenous and exogenous Gata4 expression in representative iGata4 clone after different time points of DOX treatment in 2i/Lif. **J**, RT-PCR analysis for primitive endoderm markers Pdgfra, Gata4, Gata6 and Sox17 expression in iGata4 clone cultured in primed or naïve conditions and induced with DOX for 24h in the same conditions. Values are normalized to Actin and/or Gapdh, compared to naïve 2i/Lif ESCs. One-Way ANOVA; *p Value < 0.05; ** p Value < 0.005; *** p Value < 0.0005; **** p Value < 0.0001; ns, not significant.

Figure S2. Optimization of sEmbryos culture conditions (Related to Figure 2)

A, The different fluorescently labeled donor naïve ESC populations are indicated and used for co-

aggregation as in **Figure 1D**. Representative examples of abnormally assembled sEmbryos at day 4 compared to properly patterned sEmbryos at this stage (Right side). **B,** Normally developed whole sEmbryo at day 8 of the culture protocol (upper panel), further cultured to day 9 which currently leads to abnormally enlarged heart with massive pericardial effusion and no further adequate embryo proper development (lower panel). **C,** Representative examples of cell number calibration and optimization experiments for generating sEmbryos. Representative bright field images of sEmbryos at day 6 of the culture protocol assembled from different ratios and number of WT ESC, iGata4 and iCdx2 cells. White arrowheads mark properly developed egg-cylinder shaped embryos based on morphology. **D,** Representative examples of DOX induction timing calibration and optimization experiments for generating sEmbryos. Representative bright field images of sEmbryos at day 5 of culture assembled from different cell combinations and DOX pre-treatment regimens. **E,** Schematic representation of different tested parameters and protocol regimens for establishing the optimized sEmbryo culture protocol (first line represents optimized protocol with optimal sEmbryo outcome as shown for Day 5 and Day 8). Atmospheric pressure, culture media compositions, as well as usage of static, shaker or rolling culture conditions at different time-points were evaluated. Representative images of the outcome are shown (right panels). (HUS- Human umbilical cord serum, RAS- Rat Serum, IVC – in vitro culture media (with % FBS / KSR as indicated)). Scale bars are indicated on each image.

Figure S3. Images representing technical steps during sEmbryo culture protocol (Related to Figure 2)
A, Schematic depiction describing the sEmbryo culture protocol steps from day 0 to day 8 (upper panel). Representative images of 24-well Aggrewell plates used for sEmbryo static culture (Day 0 – Day 3) and sEmbryos in non-adherent 6 well plate placed on orbital shaker inside a regular tissue culture incubator at day 4. **B**, Images of sEmbryos transferred to in house generated electronically controlled rolling culture platform and glass bottles on day 5. **C,** Representative images of sEmbryos at Day 6 in the electronically controlled ex utero roller culture system. **D**, Day 5-8 representative images showing the growth of sEmbryo inside glass bottles in the ex utero roller culture system used herein.

Figure S4. sEmbryos (iCdx2) adequately express post-implantation lineage markers (Related to Figure 3)
A, Rows 1-2: Middle-section immunostaining images of Day 3 sEmbryo (iCdx2) for the epiblast marker Oct4, extraembryonic ectoderm markers Cdx2 and Ap2γ, along with visceral endoderm markers Sox17 and Gata4. Rows 3-6: Immunostaining of Day 4 sEmbryo (iCdx2) for Epi, VE and ExE markers along with E5.5 natural in utero controls. Rows 7-8: Day 5 sEmbryos (iCdx2) immunostained for different lineage specific markers and E6.5 natural in utero controls. **B**. Rows 1-2: Day 5 sEmbryos (iCdx2) immunostained

for different lineage specific markers and E6.5 natural in utero controls. Rows 3-8: Representative immunostainings for Epi, ExE and VE markers in Day 5 sEmbryos (iCdx2) alongside corresponding E6.5 natural in utero control embryos. The primitive streak in day 5 sEmbryos (iCdx2) is marked by Brachyury (Red) immunostaining, while the migrating anterior visceral endoderm at the opposite side is marked by Cer1 (magenta) and Dkk1 (yellow), similar to in utero E6.5 control. Scale bars, 50 μM. **C**, Embryonic length measurements (μm) of iCdx2 sEmbryos and matching natural embryos at the indicated timepoints. Length measurement for abnormally developed iCdx2 sEmbryos at day 8 is shown in the far-right column. Dots represent individual embryos; data are mean ± s.e.m.; n = 17 E5.5, 15 E6.5, 9 E8.5 (natural embryos); n =17 day 4, 19 day 5, 18 day 8 (sEmbryos iCdx2); n = 15 day 8 (abnormal sEmbryos); ns, not significant; two-tailed Student's t-test. **D,** Bright field images of abnormally developed iCdx2 sEmbryos at day 8 of culture protocol and adequately developed iCdx2 sEmbryos shown as reference controls (right side). Abnormalities and absent compartment are highlighted where indicated. Al, allantois; H, heart; NF, neural folds; NT, neural tube; TB, tail bud. Scale bar, 200 μM.

Figure S5. Analysis of organogenesis-stage sEmbryos at day 8 and sEmbryo formation efficiency (Related to Figure 4)

A, Bright field images exemplifying the scope of morphological variation that can be seen among day 8 sEmbryos (after dissection from the yolk sac). sEmbryos shown are obtained by aggregating WT ESCs, iGata4 ESCs and either short-term (3 day DOX) induced iCdx2 ESCs, long-term (10 day DOX) induced iCdx2 ESCs, or embryonic-derived TSCs (eTSCs) as indicated. **B,** Representative image of a random field of view exemplifying egg cylinder morphology of embryos that renders them being selected at day 5 (red arrows) for transfer into roller culture stage of the protocol. **C**, Efficiency of properly developed sEmbryos (iCdx2 + eTSCs-derived) based on lineage labeling data from **Figure 1G** (day 3 and 4), and morphology-based assessment from bright field images from day 5 to 8. Values from day 3 to 5 are calculated relative to the number of properly developed embryos per sample taken for this analysis on the same day, and percentages from day 6 to 8 are calculated relative to the number of embryos transferred to roller culture bottles on day 5 (see Methods). Values are mean ± s.e.m.; n = 7 on day 3, n= 15 on day 4, n=26 on day 5, n=61 on day 6, n= 26 on day 7, n= 26 on day 8. **D,** Calculated efficiency of properly developed sEmbryos (iCdx2 + eTSCs-derived). Values from day 3 to 5 correspond to the same values shown in panel **S5C**. The adjusted effective efficiency of properly developed sEmbryos is shown from day 6 to 8, presented as relative to the total number of starting aggregates in the experiment. data represent mean ± s.e.m.; **E**, Comparison of efficiency percentage of normally developed sEmbryos obtained using iCdx2 ESCs or eTSCs at day 6, 7 and 8 of the culture protocol, after selection and transfer to the roller culture at day 5 based on morphological criteria. The total number of embryos transferred at day 5 represents a value of 100%. Dots

represent percentage of normal embryos per bottle; data represent mean ± s.e.m.; n = 20 on day 6, n= 6 on day 7, n= 6 on day 8 (eTSCs); n = 41 on day 6, n= 20 on day 7, n=20 on day 8 (iCdx2); two-tailed Student's t-test for normally distributed data and non-parametric U Mann-Whitney test for non-normally distributed data. P values are indicated on each column. **F,** Representative whole-mount immunostaining confocal images of lineage-specific markers expressed in day 8 sEmbryos (iCdx2), compared to natural in utero E8.5 embryos. **G,** Individual sEmbryo (iCdx2) stained for Sox2 (orange), Brachyury (yellow) and MHC-II (magenta) and imaged from the dorsal, lateral and ventral sides (upper panels). An eTSCs-derived sEmbryo stained for Sox9 (red) and Sox17 (turquoise) showing the foregut invagination and notochord at the ventral side of the embryo is shown (lower panels). **H,** Two examples of representative H&E staining on sagittal histological sections displaying the morpho-histological and structural complexity similarity between day 8 sEmbryos (iCdx2) and natural in utero E8.5 embryos. Scale bars, 200 µM in A, B, E, and F, 100 in G. Al, allantois; FB, forebrain; FP, floor plate; Fg, foregut pocket; H, heart; MB, midbrain; Nc, notochord; NC, neural crest; NF, neural folds; NT, neural tube; TB, tail bud, S, somite, YS, yolk sac.

Figure S6. scRNA-seq analysis of advanced mouse synthetic embryos (Related to Figure 7)

A, Violin plots indicating the number of genes and unique molecular identifiers (UMIs) obtained per embryo type. Median of 5,680 UMIs and 2,273 genes were detected per cell. After filtering out low quality cells, median of 5,377 UMIs and 2,189 genes were detected per cell. **B**, Lineage annotation of cell clusters. Dot plots illustrating the area under the curve (AUC) enrichment value of overlapping cells across clusters and tissue lineages. Dot size denotes the magnitude of enrichment. Colors indicate P-values (Mann–Whitney test calculated from AUC score). **C**, UMAP-based plots illustrating the normalized AUC assigned value of all individual cells for each lineage on natural and synthetic embryo samples. **D**, Day 8 synthetic embryo cells (red), E8.5 natural embryo cells (black), E10.5 natural embryo cells (blue) and E6.5 natural embryo cells (green), projected on the same UMAP plot. Cell number in each graph is indicated. **E,** scRNA-seq analysis of natural embryos, in utero and ex utero versus synthetic embryos (grown ex utero). UMAP plot displaying individual cells (n = 26,946 from 9 natural in utero grown E8.5 embryos; n = 7,014 from 4 natural ex-utero E8.5 embryos; n = 40,658 from 9 sEmbryo grown ex utero. Points are colored according to their assigned cell cluster. **F**, Bar charts depicting the proportional abundance of each cell cluster in natural in-utero and ex-utero, and in synthetic embryos grown ex utero. Asterisks denote clusters with statistically significant differences between the two indicated groups. * FDR corrected t-test $p<0.1$. Colors as in (**E**).

Figure S7. scRNA-seq analysis confirms high correlation in gene expression between organogenesis-stage mouse synthetic embryos and their natural counterparts (Related to Figure 7)

A, Correlation of gene expression of 24,348 genes for each cluster between natural and synthetic embryos. Correlation coefficients are indicated. **B**, Left: Dot plots illustrating the expression of selected markers of notochord, somitic mesoderm, neural tube and cardiac tissues across selected clusters, comparing natural to synthetic embryo cells. Dot size denotes the normalized expression. Colors indicate enrichment $-\log_{10}$(p-values) (Fisher exact test). Right: Dot plots illustrating the expression of selected markers of the indicated extra-embryonic tissue across selected clusters, comparing natural (in utero and ex utero) to synthetic embryo (ex utero) cells. Dot size denotes the normalized expression. Colors indicate enrichment $-\log_{10}$(p-values) (Fisher exact test). **C**, Normalized expression of selected placental and trophoblast markers, projected on UMAP of E8.5 natural in utero embryos, E8.5 natural ex utero embryos or day 8 ex utero sEmbryos.

STAR Methods

Resource availability

Lead contact

Further information and requests for the resources and reagents may be directed to the lead corresponding author Jacob H. Hanna (Jacob.hanna@weizmann.ac.il)

Materials availability

All materials used are commercially available except for the human serum used herein. All newly generated mouse lines and plasmids are available from the lead contact with a completed Materials Transfer Agreement.

Data and code availability

All bulk and scRNA-seq data are deposited under GEO: GSE208681.

Related additional figures and data can be found on Mendeley Data (doi: 10.17632/6nhpgnxf3y.1).

This paper does not report original code. Codes used to analyze the RNA-sequencing data are available from the authors upon request. Any additional information required to reanalyze the data reported in this work is available from the lead contact upon request.

Experimental Model and Subject Details

Animals

Natural in utero developed embryos were obtained from female mice 5-8-week-old ICR or BDF1 mated with BDF1 male studs (Harlan). Insemination was verified the next morning by the presence of a copulatory plug, and this day was defined as embryonic day 0.5 (E0.5). Both male and female natural in utero and ex utero grown embryos were used without any pre-selection or preference. All animal experiments were performed according to the Animal Protection Guidelines of Weizmann Institute of Science and approved by relevant Weizmann Institute IACUC (#01390120-1, 01330120-2, 33520117-2). Healthy mice were housed in a standard 12-hour light/12-hour dark cycle conditions in a specialized and certified animal facility.

Stem cell lines

The following mouse ESC lines were used: BVSC ESC (Mixed BDF1 X B6 background; was found most efficient in yielding day 8 sEmbryos; Male ESC line), WT ICR1 ESC (ICR; Male ESC line), WT V6.5 ESCs (C57B6/129sJae; Male ESC line), and KH2-WT ESC (male ESC line) line carrying both

M2RtTa allele in the Rosa26 locus and a modified Col1 locus with an FRT site to efficiently insert Tet-ON regulated alleles as previously described (Hochedlinger et al., 2005). We note that so far in our hands, ~40-50% of ESC lines tested (including V6.5 ESC) could not generate normal synthetic embryos beyond day 6 when co-aggregated with iCdx2 and iGata4. The previously described BVSC ESC lines (Hayashi et al., 2011) carries Blimp1-mVenus and Stella-CFP (BVSC) reporter alleles for tracking PGC formation.

Embryo derived Trophoblast stem cell clonal lines (eTSC) were derived as previously described from E6.5 BDF2 embryos and expanded on irradiated MEFs in classical TSC media (Tanaka et al., 1998). Briefly, trophectoderm part was dissected and plated on irradiated mouse embryonic fibroblast with TSC media supplemented with 25 ng/ml FGF4 (Peprotech 100-31), 1 µg/ml Heparin (Sigma H3149). TSC media was changed every two days till the TSC clones were established, one of which eTSC line#11 was used in experiments described in **Figure 5** and gene expression analysis. For eTSC derivation from blastocysts of BDF2 mice, blastocysts at E3.5 were flushed from uterus and plated on irradiated mouse fibroblast in TSC media supplemented with 25 ng/ml recombinant FGF4 (Peprotech 100-31), 1µg/ml Heparin (Sigma H3149). On day 3, blastocysts hatched, attached on the plate and small outgrowth was observed. On day 5-7, the blastocyst outgrowth was disaggregated using 0.25% Trypsin-EDTA (Biological Industries – Sartorius 03-050-1B). After day 7 flat epithelial sheet like morphology TSC colonies were observed. TSC media was replaced every two days. Two blastocysts derived eTSC named eTSC line #2 and eTSC line #5 were used as controls for comparative bulk RNA-seq gene expression analysis.

Mouse XEN lines were derived in house from ICR blastocysts as previously described (Anderson et al., 2017). Briefly, E3.5 blastocysts were flushed from the uterus and plated on irradiated mouse fibroblast in TSC media supplemented with 25 ng/ml FGF4 (Peprotech 100-31), 1µg/ml Heparin (Sigma H3149). On day 3, blastocysts hatched, attached on the plate and small outgrowths were observed. From day 10-15 XEN clones were observed and manually picked. Once XEN clones and lines were established, FGF4 and heparin were no longer needed and omitted from maintenance media. Validated XEN line #7 was used in this study.

Method Details

Naïve ESC and other stem cell line in vitro culture conditions

Golden stocks of mouse ESCs were cultured on feeder layer of irradiated mouse embryonic fibroblast (MEFs) and maintained (and gene targeted when relevant) in conventional mouse ES medium (Serum/Lif) composed of 1x DMEM (GIBCO 41965) supplemented with 20% FBS (heat inactivated and filtered), 1mM GlutaMAX (GIBCO, 35050061), 1% penicillin streptomycin (Biological Industries – Sartorius 03-031-1B), 1% Sodium Pyruvate (Biological Industries – Sartorius 03-042-1B), 1% nonessential amino acids (Biological Industries – Sartorius 01-340-1B), 0.1 mM β-mercaptoethanol (Thermo

31350010), 10 ng/ml recombinant human Lif (in-house prepared). Serum/Lif conditions were used to maintain "golden" stocks since they do not yield global erosion and loss of imprinting as seen upon long term expansion in serum free 2i/Lif conditions (Choi et al., 2017).

To convert them into naïve ESCs in 2i/Lif conditions, ESCs were maintained and expanded in serum-free chemically defined N2B27-based media: 240 ml Neurobasal (Thermo 21103049) and 240 ml of DMEM-F12 with HEPES (SIGMA D6421), 5 ml N2 supplement (Invitrogen; 17502048), 5 ml B27 supplement (Invitrogen; 17504044 or in house prepared), 1mM GlutaMAX (GIBCO, 35050061), 1% nonessential amino acids (Biological Industries – Sartorius 01-340-1B), 0.1 mM β-mercaptoethanol (Thermo 31350010), 1% penicillin-streptomycin (Biological Industries – Sartorius 03-031-1B). Naïve 2i/Lif conditions for murine PSCs included 20 ng/ml recombinant human Lif (in-house made), small-molecule inhibitors CHIR99021 (CHIR, 3μM- Axon Medchem 1386) and PD0325901 (PD, 1μM – Axon Medchem 1408) (referred to as 2i). Murine naïve ESCs were expanded on feeder layer (MEFs) or on 0.2% gelatin-coated plates. At least three passages in 2i/Lif conditions were applied before initiation of experimentation. When possible, we used mouse naïve ESC lines up to 12 passages in 2i/Lif conditions as the frequency of chromosomal abnormalities and global loss of imprinting naturally occurring in 2i/Lif conditions are still relatively lower than in higher passages (Choi et al., 2017). For maintenance of ESCs in 2i/Lif conditions, cells were passaged with trypsinization every 3-5 days.

eTSC clones and lines were plated on irradiated mouse embryonic fibroblast (MEF) layer and maintained in basal TSC media (TSCm) composed of RPMI1640 (GIBCO 21875) supplemented with 20% FBS (Sigma F7524), 1mM GlutaMAX (GIBCO, 35050061), 1% penicillin streptomycin (Biological Industries – Sartorius 03-031-1B), 1% Sodium Pyruvate (Invitrogen), 1% nonessential amino acids (Biological Industries – Sartorius 01-340-1B), 0.1 mM β-mercaptoethanol (Thermo 31350010) and supplemented with 25 ng/ml FGF4 (Peprotech 100-31), 1μg/ml Heparin (Sigma H3149). XEN clones were cultured on irradiated fibroblast layer and maintain in basal TSC media. Cells were passaged every 3-4 days when reached 70%-80% confluency. For maintenance eTSC were passaged with 0.25% trypsinization every 3-5 days. All cell lines were routinely checked for Mycoplasma contaminations every month (Lonza–MycoAlert KIT), and all samples analyzed in this study were not contaminated. This study did not conduct blinding of cell lines, data or animals used. This study did not conduct randomization of cell lines, data or animals used.

Generation of iGata4 and iCdx2 ESCs clones

We used the KH2 collagen flip-in ESC system that carriers M2RtTa allele in the Rosa26 locus (Hochedlinger et al., 2005), and flipped-in Cdx2 into the collagen locus under the regulation of Doxycycline

(DOX) inducible Tet-On promoter. KH2-Cdx2 cells (iCdx2 ESCs) changed their morphology when placed in TSCs media (TSCm) with DOX rapidly within 24-48 hours, and established TSC line after multiple passages (**Figure S1A**). iCdx2 ESC were subjected to another round of targeting to introduce an Elf5-YFP reporter allele, which is a reliable marker for TSC induction efficiency. KH2-WT ESC were co-transfected with either mouse Tet-On Gata4 construct or mouse Tet-On Cdx2 construct along with flippase recombinase construct (Hochedlinger et al., 2005). Hygromycin (150ug/ml) antibiotic selection was applied for 1 week to 10 days. Resistant clones were picked and cultured for downstream characterization. PCR for genomic DNA to confirm cassette insertion were done. Functional validation of correctly targeted clones was subsequently done by RT-PCR and immunostaining for specific DOX induction. Multiple targeted clones that showed DOX induced Cdx2 overexpression were validated for correct targeting and interchangeably used with similar outcome throughout the study. Detailed generation, characterization and validation of these lines can be found on related figures deposited on Mendeley Data (Hanna, Jacob (2022), "Post-Gastrulation Synthetic Embryos Generated Ex Utero Solely from Naïve ESCs", Mendeley Data (doi: 10.17632/6nhpgnxf3y.1)).

Generation of Elf5-EYFP reporter iCdx2 ESCs

iCdx2 (KH2-Cdx2) validated clone 3 was used for CRISPR targeting EYFP in 3' end of mouse Elf5 gene. Cells we co transfected with previously generated targeting plasmid (Addgene #128833) and guide RNA plasmid (#128836). Following neomycin and ganciclovir antibiotic selection for 10 days, total clonal population was transfected with Cre and subcloned. Single cell clones were validated for correct insertion. At 3' end using forward ATGGTCCTGCTGGAGTTCGTGAC and reverse TGGTCCATCTGCTTGTAGGCAAGA primer pair, and at 5' end using forward TTCACCTTTGAAGCTAATCGTTTGAGG and reverse AACTTGTGGCCGTTTACGTCGC primer pair. Correctly targeted clones were further validated for off-target insertions by Southern blot analysis.

Generation of fluorescent labeled ESCs

KH2 WT ESCs, KH2-Gata4 clone 7 (iGata4) and KH2-Cdx2 clone 3 (iCdx2) were transduced with lentivirus particles constitutively expressing either fluorescent BFP, GFP or mCherry proteins, respectively. For the generation of lentivirus, HEK293T cells were plated in 10 ml DMEM, containing 10% FBS and Pen/Strep in 10 cm dishes, in aliquots of 5.5 million cells per well. On the next day, cells were transfected with the third-generation lentiviral vectors ((0.8 μg of pRSV-Rev (Addgene 12253), 0.8 μg of pMDLg/pRRE (Addgene 12251), 1.6 μg of pMD2.G (Addgene12259)), using jetPEI transfection reagent, along with 16 μg of the target plasmid of each transduced fluorescent proteins BFP, GFP and mCherry. The supernatant containing the virus was collected 48hr and 72hr following transfection, filtered using 0.45 μm

filter. ESCs were plated in Serum/Lif condition on gelatin coated 6-well plates at low density and transduced with lentivirus in the presence of protamine sulfate (8µg/ml). 48hr later the infected ESCs were expanded for 1-3 passages and sorted for positive population and further expanded for experimentation.

Human umbilical cord serum (HUS) and human adult serum (HAS)

Collection of human cord blood serum foe ex utero culture of embryos was done as described previously (Aguilera-Castrejon et al., 2021) following the guidelines approved by Rambam Medical Center Helsinki committee (#RMB-0452-15). Healthy women over the age of 18 and under 40 who gave their consent and were scheduled for caesarian section delivery were eligible for cord blood collection. Blood was manually drawn by the obstetrician surgeon, using a large bore 14-gauge needle and a 50mL syringe, directly from the umbilical cord. Serum extraction must be conducted within 2hours of blood donation, to avoid byproducts of hemolysis which are highly toxic to embryos and embryo-like entities. Blood was collected and quickly distributed to 5/8 mL pro-coagulant sterile test tubes (Greiner Bio-One, Z Serum Sep Clot Activator, #456005) and cooled to 4°C for 15 minutes, followed by centrifugation at 2500G for 10 minutes at 4°C. Tubes showing signs of hemolysis were discarded. Serum was filtered through a 0.22 µM filter (Nalgene, Ref # 565-0020), heat-inactivated at 55°C in a water bath for 45 minutes and immediately aliquoted and stored at -80°C for up to six months. Human adult blood serum (HAS) can replace HUS to generate mouse sEmbryos at comparable efficiency and quality. HAS was collected from freshly donated blood from male and female healthy adult donors and isolated following the protocol described above for HUS.

Electronically controlled ex utero roller culture platform

Putative sEmbryos were kept starting from Day 5 in the ex utero electronically controlled roller culture platform (Aguilera-Castrejon et al., 2021). A 'rotator' culture method provides continuous flow of oxygenating gas to cultures in rotating bottles (BTC Rotating Bottle Culture Unit BTC 02 model by B.T.C. Engineering, – Cullum Starr Precision Engineering Ltd - UK). sEmbryos are kept on a rotating bottles culture unit inside a “precision” incubator system (BTC01 model with gas bubbler kit - by B.T.C. Engineering, – Cullum Starr Precision Engineering Ltd - UK) during all the time of culture. Glass culture bottles (BTC 04) are plugged into the hollowed rotating drum. Oxygenating gas flows along the axis and is distributed to the culture bottles by a baffle plate within the drum. The rotator is supplied complete with gas filter, bubbler and leads by the manufacturer. The BTC Precision Incubator uses a thyristor-controlled heater and high flow-rate fan to give a highly stable and uniform temperature. The incubator has a working volume 370 x 350 x 200mm high which is accessed through the hinged Perspex top. The heater element is rated at 750 Watts. Bung (Hole) BTC 06 is used to seal the bottles and Bung (Solid) BTC 07 is used to seal

the drum (B.T.C. Engineering, – Cullum Starr Precision Engineering Ltd – UK). In order to achieve constant O_2 and CO_2 levels in the culture medium throughout the incubation period, the incubator module was linked to an in-house designed and customized gas and pressure electronic control unit (models#-HannaLab1 or HannaLab1.2; designed by the Hanna lab and assembled by Arad Technologies LTD, Ashdod, Israel) (Aguilera-Castrejon et al., 2021). Carbon dioxide and oxygen concentration are regulated by specific controllers located inside the regulation module. A pressure transmitter allows precise and stable control of the gas pressure between 5 to 10 psi (positive pressure over ambient external atmospheric pressure), that is transmitted to the embryo bottle apparatus. Regulation of pressure generated by the pressure pump is done by setting the adequate voltage on the pressure transmitter. Oxygen and CO_2 are then injected into the gas mixer box. The mixing of the gases in the gas box is homogeneous and mixed by a centrifugal blower. The gases are injected into the incubator at pressure of ~6.5-8 psi (which was found as the optimal level) by a pump. Adequate and stable control of the pressure of the gas flowing from the mixing box outlet into the water bottle inside the incubator should be measured by using a pressure gauge before each experiment. The main components of the system are the following: Oxygen and CO_2 controller, pressure pump, vacuum pump, oxygen and CO_2 sensors, power supply, check valve, mix gas box, pressure transmitter, limit flow, adapter control for gases, 1 µm filters, centrifugal blower. Gas flows from the mix box through the inlet into the water bottle, and the speed of gas flowing into the bottle can be controlled with a valve on the lid of the water bottle. The bubble rate (which indicates the speed of gas flowing into the bottles) can be adjusted as needed by the user by closing/opening the valve. Ideally, the flow of bubbles should be such to allow formation of individual bubbles at a rate of 3-4 bubbles per second in the water-filled test tube outlet, or to the first point where continuous bubbling is observed (**Supplementary Video S4**). Humidified gas circulates to a glass test tube and then to the inside of the bottles in the rotating drum. Gas flow speed can be monitored by the rate of bubbles created inside the outlet water-filled test tube. A black nontransparent cloth is used cover the incubator to provide phototoxicity protection for the ex utero cultured embryos and sEmbryos.

Naïve ESC-derived synthetic embryo ex utero culture

To generate post-gastrulation mouse sEmbryos from naïve ESCs, AggreWell 24-well plate 400 (STEMCELL Technologies 34415), or AggreWell 24-well plate 800 (STEMCELL Technologies 34815) were used with comparable outcome. AggreWell plate preparation was done according to manufacturer instructions. Briefly, 500 ul of anti-adherence rinsing solution (STEMCELL Technologies 07010) was added to each well. Plate was centrifuged at 2,000g for 5 minutes and incubated 30 min at room temperature. After incubation, rinsing solution was removed and the plate was washed twice with PBS. 500 µl of aggregation media (AM) supplemented with DOX (2 µg/ml final concentration - Sigma D9891) and ROCKi

Y27632 (5nM final concentration - Axon Medchem 1683; up to 2000nM can be safely used) was added to each well. Aggregation Media (**AM**): 1x DMEM (GIBCO-41965) supplemented with 20% FBS (Sigma), 1 mM GlutaMAX (GIBCO, 35050061), 1% penicillin streptomycin (Biological Industries – Sartorius 03-031-1B), 1% Sodium Pyruvate (Biological Industries – Sartorius 03-042-1B), 1% non-essential amino acids (Biological Industries – Sartorius 01-340-1B) and 0.1 mM β-mercaptoethanol (Thermo 31350010).

For synthetic embryos generated solely from naïve ESCs starting populations (termed **iCdx2 sEmbryos)** the following three kinds of cells were co-aggregated: naïve WT ESCs (either BVSC, ICR, KH2-WT or V6.5 ESC) in 2i/Lif, naïve iGata4 ESCs in 2i/Lif, naïve iCdx2 ESCs in 2i/Lif. For synthetic embryos generated by using embryo derived TSC lines (eTSC) instead of iCdx2 cells (termed **eTSC sEmbryos)**, the following three stem cell populations were co-aggregated: naïve WT ESCs (either KH2-WT, BVSC or V6.5 ESCs) in 2i/Lif, naïve iGata4 ESCs in 2i/Lif, and eTSC grown in TSCm.

To prepare ESCs for iCdx2 sEmbryos generation, naïve KH2 Gata4 ESCs (iGata4) cultured in 2i/Lif media were treated with DOX (2µg/ml- Sigma D9891) in 2i/Lif or in aggregation media (AM) for 24hr before starting the experiment. Naïve KH2 Cdx2 ESCs (iCdx2) cultured in 2i/Lif were treated with DOX (2µg/ml- Sigma D9891) for different time points (-1 day to -14 days) in TSC media (25 ng/ml FGF4 (Peprotech), 1µg/ml Heparin (Sigma)) supplemented with lysophosphatidic acid (LPA) 0.5-1 µM, which is a Hippo pathway inhibitor. Non-inducible WT ESC fraction did not undergo special pre-treatment and continued to be maintained in 2i/Lif conditions until harvesting for coaggregation.

For preparation of eTSC sEmbryos, naïve KH2 Gata4 ESCs cultured in 2i/Lif media were treated with DOX (2µg/ml- Sigma D9891) in 2i/Lif or in Aggregation Media (AM) for 24hr before starting the experiment. Non-inducible WT ESC fraction did not undergo special pre-treatment and continued to be maintained in 2i/Lif conditions. eTSC lines did not undergo pre-treatment and were maintained in TSC media (TSCm).

At the day of aggregation (day 0), the three donor cell populations were trypsinized with 0.05% trypsin-EDTA solution (Biological Industries – Sartorius 03-053-1B) for 4-6 minutes at 37^{o}C. Trypsin enzymatic reaction was stopped by adding Aggregation Media (AM). Cells were centrifuged at 1200 rpm for 3 minutes and resuspended in AM with DOX (2µg/ml- Sigma D9891) and ROCKi Y27632 (5nM final concentration - Axon Medchem 1683). Cells were plated on gelatinized tissue culture plates for mouse embryonic fibroblast depletion for 20 min at 37^{o}C. Supernatant was collected, centrifuged and cells were resuspended. The three cell fractions were counted and resuspended in AM with DOX (2µg/ml- Sigma D9891) and ROCKi Y27632 (5nM - Axon Medchem 1683). A ratio of (1 WT-ESC: 1 iGata4 ESC: 3.33 iCdx2 ESC or eTSC) was maintained in aggregation experiments with the following exact number of cells depending on the aggregation plate used: A) Aggrewell 800: Number of microwells per well in 24 well plate = 300; Number of added cells per each well of a 24 well plate = iCdx2: 5000 cells + iGata4: 1500

cells + WT ESC 1500 cells; Number of Cells per single microwell = ~27 cells. B) Aggrewell 400: Number of microwells per well in 24 well plate = 1200; Number of added cells per each well of a 24 well plate = iCdx2: 20000 cells + iGata4: 6000 cells + WT ESC 6000 cells; Number of Cells per single microwell = ~27 cells. Similar cell number parameters were used when using eTSC instead of iCdx2.

1 ml of cell-mix suspension was gently added dropwise to each well of the AggreWell plate followed by centrifugation at 700 rpm (100g) for 3 minutes and incubation at 37^{o}C (total end volume is 1.5ml). Next day (day 1), 1 ml of media (out of total 1.5 ml) was gently removed from each well and replaced with 1ml of preheated AM media with DOX (2µg/ml- Sigma D9891). On day 2, 1 ml of media was removed from each well and replaced with 1 ml of preheated AM. On day 3, 1 ml of media was removed from each well and replaced with 1 ml of preheated EUCM2 media. **EUCM2** (a modified version of IVC media (Bedzhov and Zernicka-Goetz, 2014) and that avoids integrating KSR at any step as it is highly prohibitive for a successful outcome): Advanced DMEM/F12 (GIBCO 21331-020), extra added 1 mM Sodium pyruvate (Sigma-Aldrich, S8636), 0.5% CMRL media (GIBCO 11530037), extra added 1 mg/ml D(+)-Glucose Monohydrate (J.T. Baker - 0113) (e.g. add 500mg per 500ml media), 100 nM T3 (3,3′,5-Triiodo-L-thyronine sodium salt) (Sigma-Aldrich, T6397), 1 mM GlutaMAX (GIBCO, 35050061), 1% penicillin streptomycin (Biological Industries – Sartorius 03-031-1B), 1x of ITS-X supplement (Thermo Fisher Scientific 51500-056), 8 nM B-estradiol (Sigma-Aldrich, E8875), 200 ng/ml progesterone (Sigma-Aldrich, P0130), 25 µM N-acetyl-L-cysteine (Sigma-Aldrich, A7250), 30% FBS (Sigma Aldrich F7524 – heat inactivated and filtered).

At day 4, sEmbryos were gently transferred to 6-well cell suspension culture plate (Greiner, 657185) with 5 ml of preheated EUCM2 per well and placed on shaker rotation 60 rpm/min (Thermo 88881102 + 88881123). On day 5, egg cylinder-shape sEmbryos were picked and transferred to glass culture bottles (30-50 sEmbryos per bottle) containing 2 mL of freshly prepared ex utero culture media (EUCM). The bottles were placed on the rolling culture system, rotating at 30 revolutions per minute at 37^{o}C, and continuously gassed with an atmosphere of 21% O_2, 5% CO_2 at 6.5-8 pounds per square inch (psi).

From day 6 to day 8, 1 ml of EUCM was replaced with 1 ml of freshly prepared preheated EUCM and kept on rolling culture system. EUCM (also known as EUCM1) is composed of 25% DMEM (GIBCO 11880 – DMEM, low glucose, pyruvate, no glutamine, no phenol red (and no HEPES)) plus 50% Rat Serum (RAS) (ENVIGO Bioproducts, B-4520) and 25% Human Umbilical Cord Blood Serum (HUS) (or Human Adult Blood Serum (HAS)) that is prepared in-house, and supplemented with a final concentration of 1x GlutaMAX (GIBCO, 35050061), 50 units/ml penicillin - 50µg/ml streptomycin (Biological industries, 030311B), 1 mM sodium pyruvate (Biological industries, 030421B), extra added 4 mg/mL of D-glucose (J.T. Baker), and added HEPES (11 mM final concentration) (GIBCO 15630056). Rat serum is stored at -

80°C and heat inactivated at 56°C for half an hour and filtered through a 0.22 µm PVDF filter (Millipore; SLGV033RS) prior to use. RAS and HUS/HAS should be freshly thawed and used immediately before experimentation. RAS and HUS can be thawed/frozen once. Culture media was pre-heated for at least an hour by placing it inside a glass bottle on the rotating culture. Please see **Supplementary Videos S3-5** for further details and technical demonstrations.

Whole-mount immunostaining of sEmbryos

sEmbryos grown ex utero and equivalent in utero natural embryo controls were fixed with 4% PFA EM grade (Electron microscopy sciences, 15710) in PBS at 4°C over-night. Natural embryos were dissected removing the Reichert's membrane for E6.5-E7.5 embryos, or the yolk sac and amnion for E8.5 embryos and washed once with 1×PBS before fixation. sEmbryos were then washed in PBS for 5 minutes 3 times, permeabilized in PBS with 0.5% Triton X-100/0.1 M glycine for 30 minutes, blocked with 10% normal donkey serum/0.1% Triton X-100 in PBS for 1 hour at room temperature (RT), and incubated over-night at 4°C with primary antibodies, diluted in blocking solution. After, embryos were rinsed 3 times for 5 minutes each in PBS/0.2% TritonX-100, incubated for 2 hours at room temperature with secondary antibodies diluted 1:200 in blocking solution (all secondary antibodies were from Jackson ImmunoResearch), counterstained with DAPI (1 µg/ml in PBS) for 10 minutes, and washed with PBS for 5 minutes 3 times. Yolk sacs isolated from natural and synthetic embryos were fixed and stained following this protocol. The primary antibodies used are listed in key source table.

Immunohistochemistry and histological analysis

For OCT-sectioning, sEmbryos day 8 were fixed overnight in 4% PFA at 4°C, washed three times in PBS for 10 min each and submerged first in 15% Sucrose/PBS and then 30% Sucrose overnight at 4°C. The day after, samples were subjected to increasing gradient of OCT concentration in Sucrose/PBS followed by embedding in OCT on dry ice and stored at - 80°C until further processing. Cryoblocks were cut with LEICA CM1950 and washed once with 1xPBS and incubated with 0.3% H_2O_2 for 20 min. After permeabilization with 0.1% Triton X-100 in PBS for 10 min., slides were again washed three times with 1xPBS for 2 min. each and blocked in 10% normal donkey serum in PBS in humidified chamber for 20 min. at RT. Slides were then incubated with proper primary antibody diluted in antibody solution (1% BSA in 0.1% Triton X-100) at 4 °C overnight. Sections were then washed three times (5 min each) in 0.1% Triton X-100 in PBS, incubated with appropriate secondary antibodies diluted in antibody solution at RT for 1 h in the dark, counterstained with DAPI for 20 min and mounted with Shandon Immuno-Mount (Thermo Scientific, 9990412). The primary antibodies used are listed in key source table. For Day 8 sEmbryos histological analysis, transversal and sagittal OCT sections slides were stained with hematoxylin

and eosin. In utero E8.5 natural embryo were used as reference control for histological examinations. All histology results and examination were confirmed by a certified pathologist (Dr. Ori Brenner).

Confocal microscopy

Whole-mount immunofluorescence and immunohistochemistry images were acquired with a Zeiss LSM 700 inverted confocal microscope (Zeiss) equipped with 405nm, 488nm, 555nm and 635nm solid state lasers, using a Plan-Apochromat 20× air objective (numerical aperture 0.8) for E5.5/E6.5 natural embryos and for day 3-6 sEmbryos, and an EC Plan Neofluar 10× air objective (numerical aperture 0.3) for E8.5 natural embryos and day 8 sEmbryos. Images were acquired at 1024×1024 resolution. All images were acquired within the following range of parameters: Laser power: 405 nm: 10-20%; 488 nm: 5-30%; 555nm 10-40%; 635 nm: 30-80%. Gain ranged from 350 to 600. Pixel size was 1.25 µm with a z-step of 15 µm when using the 10× objective, or 0.5 µm with z-step of 5 µm when using the 20× objective. For confocal imaging sEmbryos were mounted in 35mm glass bottom dishes (In Vitro Scientific, D35201.5N). Images and maximum intensity projections were processed using Zen 2 blue edition software 2011 (Zeiss) and Adobe Photoshop CS4. Throughout the paper, insets are enlargements of the dashed boxes as indicated. Throughout the manuscript images are representative of a minimum of 3 independent biological replicates.

Morphological evaluation of mouse early development and efficiency calculations

Assessment of appropriate embryo development was performed based on previously defined morphological features for natural and stem-cell derived embryos and as done in (Aguilera-Castrejon et al., 2021). Between day 4 to 5, correctly assembled sEmbryos are constituted by three clearly segregated lineages: the cup-shaped epiblast (Epi), the extraembryonic ectoderm (ExE) and the visceral endoderm (VE) which surrounds the Epi and ExE. The epiblast and ExE present a unified amniotic cavity. At day 5 the sEmbryos break radial symmetry of the epiblast and the primitive streak appears. At day 6, properly developed embryos reach the neural plate stage equivalent to E7.5. Presence of the amnion at the middle of the cylinder divides the amniotic and exocoelomic cavities, and a small allantois bud at the base of the primitive streak can be observed in some of the sEmbryos. The most prominent feature at day 7 is the formation the neural groove by the anterior ectoderm. On the last culture day (day 8), the sEmbryos grow enclosed inside the yolk sac and amnion and develop prominent neural folds and neural tube at the dorsal side, as well as invaginating foregut pocket and beating heart at the ventral part. The embryos are slightly curved dorsally and display between 1-4 somite pairs, the yolk sac blood circulation becomes evident, and the allantois is extended into the exocoelom to start fusing with the placental cone. Only embryos presenting all of the previously defined features were considered as developed properly.

The morphological parameters defined above along with spatial segregation of fluorescently-labeled cells are used throughout the manuscript for evaluating efficiency at different time-points. From day 3 to Day 5 the efficiency percentage of proper sEmbryo development is calculated based on the number of properly developed sEmbryos observed per random field of view from random wells with sEmbryos sampled on the same day. Efficiency percentages from day 6 to 8 are measured by counting the number of properly developed sEmbryos per bottle, considering and relative to the total number of aggregates transferred to each roller culture bottle at day 5 as 100%. Alternatively, estimated efficiency presented in **Figure S6D** was calculated for day 6-8 by multiplying the percentage of properly developed embryos per bottle by the average efficiency of day 5 (the day of selection of the transferred sEmbryos), and thus yielding estimated efficiency relative to the total initial starting number of aggregates in the experiment. Efficiency of antero-posterior axis establishment in egg cylinder sEmbryos was assessed based on the presence of the neural plate in one side sEmbryos at day 6 of development, out of the total number of egg cylinder embryos obtained per bottle on the same time point.

Assessment of sEmbryo length

Morphometric measurements were performed using bright field images of sEmbryos at the indicated time points. Length of the proximal-distal axis was measured for sEmbryos at both day 4 and day 5, while the antero-posterior axis was measured for sEmbryos at day 8. Measurements were performed using the CellSens Entry software (Olympus). Length of control natural embryos was used for comparison at matched embryonic stages as indicated.

Yolk sac erythroid progenitor staining

Day 8 sEmbryos (iCdx2 and eTSC) and natural E8.5 derived yolk sacs were dissected. Single cells flow cytometry staining was done using MacsQuant VYB instrument (Miltenyi, Bergisch Gladbach, Germany). Data were analyzed with FlowJo. Staining was for 30 min at 4 °C in flow cytometry buffer (PBS, 10% fetal bovine serum and 0.02% azide). For erythroid progenitor staining, we used a mouse Lineage Cell Detection Cocktail-Biotin, containing CD4, CD8, B22, CD11b, GR-1 and Ter119 (Miltenyi, Cat# 130-092-613), together with anti-cKit APC (2B8), CD41 VG (MRW), CD45 PE (30-F11) (all from Biolegend) and CD34 PB (RAM34, eBioscience) as previously described (Iturri et al., 2021). As secondary conjugated antibody we used Streptavidin-PE-Cy7 (Biolegend).

Erythroid colony forming assay

Harvested cells from day 8 sEmbryos or E8.5 yolk sacs were prepared as single cell suspension in Iscove's modified Dulbecco's medium supplemented with 2% FBS (GIBCO) and 1% penicillin

streptomycin (Invitrogen). Isolated cells were plated in triplicate at a density of ($1*10^6$) cells per 1.1 ml of MethoCult medium (Stem Cell Technologies, ™ SF M3436) in 35-mm dish and maintained at 37°C with 5% CO_2 for 12 days before being scored for primitive erythroid colonies. Colonies were visualized and validated with a bright field microscope A1 microscope (Zeiss).

RNA extraction & RT-PCR analysis

Total RNA was isolated using RNeasy mini kit (Qiagen) following manufacturer instructions. 1 µg of total RNA was reverse transcribed using a High-Capacity Reverse Transcription Kit (Applied Biosystems). RT-PCR was performed in triplicate using SYBR Green PCR Master Mix (Qiagen) and run on Viia7 platform (Applied Biosystems). Values were normalization to Actin and/or Gapdh across all experiments, data presented as fold difference compared reference sample set as 1. RT- PCR primer list used listed in **Supplementary Spreadsheet 2**.

Bulk RNA-seq (Bulk MARS-seq)

RNA-seq libraries were prepared at the crown genomics institute of the Nancy and Stephen Grand Israel National Center for Personalized Medicine, Weizmann Institute of Science. A bulk adaptation of the MARS-Seq protocol (Keren-Shaul et al. 2019) was used to generate RNA-Seq libraries for expression profiling different samples (3 biological replicates from each) (**Supplementary Spreadsheet 1**), representing different time point inductions of iCdx2 clone#3 in TSC media supplemented with or without lysophosphatidic acid (LPA) 0.5uM, KH2 WT naïve 2i-Lif ESCs, eTSC line #11 derived from post implantation E6.5 embryo, two clones of eTSCs derived from E3.5 BDF2 blastocysts, XEN clonal line derived from blastocyst and mouse embryonic fibroblast (MEFs) control. Briefly, 60 ng of input RNA from each sample was barcoded during reverse transcription and pooled. Following Agencourct Ampure XP beads cleanup (Beckman Coulter), the pooled samples underwent second strand synthesis and were linearly amplified by T7 in vitro transcription. The resulting RNA was fragmented and converted into a sequencing-ready library by tagging the samples with Illumina sequences during ligation, RT, and PCR. Libraries were quantified by Qubit and TapeStation as previously described (Keren-Shaul et al. 2019). Sequencing was done on a NovaSeq600 using an SP 100 cycles kit (Illumina).

Bulk RNA-seq analysis

Samples were analyzed using UTAP software. Reads were trimmed using CutAdapt (Martin 2011) (parameters: -a ADAPTER1 -a “A{10}” -a “T{10}” -A “A{10}” -A “T{10}” –times 2 -u 3 -u -3 -q 20 -m 25). Reads were mapped to genome mm10 using STAR v2.4.2a (parameters: –alignEndsType EndToEnd, –outFilterMismatchNoverLmax 0.05, –twopassMode Basic -alignSoftClipAtReferenceEnds no).

Sample counting was done using STAR, quantifying mm10 RefSeq annotated genes. Further analysis was done for genes having a minimum of five reads in at least one sample. Normalization of the counts and differential expression analysis was performed using DESeq2 (Love et al. 2014) with the parameters betaPrior = true, cooksCutoff = false, and independentFiltering = false. Raw P-values were adjusted for multiple testing using the procedure of Benjamini and Hochberg. Hierarchical clustering was generated in UTAP software. Expression heatmap was generated using R pheatmap package. The normalized expression levels are available in **Supplementary Spreadsheet 1**.

10X single cell RNA-seq

E8.5 natural embryos grown in utero and day 8 sEmbryos grown ex utero were selected and harvested for single cell RNA-sequencing (**Supplementary Spreadsheet 1**). All sEmbryos analyzed by scRNA-seq were generated by co-aggregating BVSC ESC lines with iCdx2+iGata4 ESCs that have a different genetic background, so that the embryonic and extra-embryonic parts will not be genetically identical in sEmbryos. Four pooled samples of sEmbryos were sequenced, one sample represents sEmbryo (iCDX2) short term DOX induced (from Day-1 until Day +1), two samples represent sEmbryo (iCDX2) 10 day dox induced (from Day -8 until Day +1) and one sample represents sEmbryo (eTSC). Moreover, to obtain sampling of single embryo single cell RNA-seq (rather than relying only on pooled samples 2 embryos), a single sEmbryo from short term induced iCdx2 was processed and sequenced. All five sEmbryo samples were processed including extraembryonic compartments without any dissection. sEmbryos were dissociated using Trypsin-EDTA solution A 0.25% (Biological Industries; 030501B). Trypsin was neutralized with media including 10% FBS and cells were washed and resuspended in 1x PBS with 400 µg/ml BSA. Cell suspension was filtered with a 100 µm cell strainer to remove cell clumps. A percentage of cell viability higher than 90% was determined by trypan blue staining. Cells were diluted at a final concentration of 1000 cells/µL. scRNA-seq libraries were generated using the 10x Genomics Chromium v3.1 Dual Index system (5000 cell target cell recovery) and sequenced using Illumina NovaSeq 6000 platform according to the manufacturer's instructions.

10X Single cell RNA-seq analysis

10x Genomics data analysis was performed using Cell Ranger 7.0 software (10x Genomics) for pre-processing of raw sequencing data, and Seurat 3.6.3 for downstream analysis. The mm10-3.0.0 gene set downloaded from 10x was used for gene reference requirements. To filter out low-expressing single cells, possible doublets produced during the 10x sample processing, or single cells with extensive mitochondrial expression, we filtered out cells with under 200 expressing genes, over 4,000 expressing genes and over 15% mitochondrial gene expression. Seurat integrated analysis and anchoring of all

individual samples was performed and then normalized by log-normalization using a scale-factor of 10,000. The top 2,000 variable genes were identified by the variance stabilizing transformation method, and subsequently scaled and centered. Principal components analysis was performed for dimensional examination using the 'elbow' method. The first 15 dimensions showed the majority of data variability. Therefore, UMAP dimensional reduction was performed on the first 15 dimensions in all samples. Clusters were detected using Seurat Find Clusters function, with resolution parameter =0.6. The number of filtered cells in each sample slightly varies between analyses that were done on different sample sets.

For cluster annotation, we used the area under the curve (AUC) methodology to identify the enrichment of each annotated gene-set to each individual single cell. The annotations were based on published gene annotations (Ibarra-Soria et al., 2018), and performed using the R package AUCELL 1.8.0, using parameters: aucMaxRank = 100 (5% of the total gene count) under the AUCell_calcAUC function. Each cell was then annotated to a single tissue based on its highest AUC score prediction. Each tissue was then cross-tabulated with each cluster to assess cluster–tissue overlap, and additionally normalized by z-score and ranged to 0–1 for plotting purposes. Next, to evaluate the probability of a certain cluster being enriched in a certain tissue, we used the annotated AUC predictions of each cell to a tissue to compare to our observed cluster annotation of each cell, thus producing a P value based on Mann–Whitney U statistics. This was calculated using the R package verification v1.42 'roc.area' function. Integration of both the predicted annotation overlap and its statistical enrichment to each cluster resulted in a predicted tissue per cluster. T-test was used to assess significant changes in the proportional size of each cluster between natural and synthetic embryos. Expression pattern of selected genes was shown as two parameters: normalized mean expression, and enrichment of cells that express this gene (expression>0), among the specified cluster (either in natural or in synthetic originated cells). Previously published E6.5 in utero grown natural embryos (Chan et al. 2019), E10.5 in utero grown embryos and E8.5 natural embryos grown ex utero by our group with the same extraction and processing method (Aguilera-Castrejon et al., 2021), were used for comparative analysis as indicted. Expression of selected TSC/placental markers was plotted on the corresponding UMAPs using SEURAT package. Notably, PGCs were not detected as separate cell cluster by scRNA-seq in either natural or synthetic embryos samples, due to being a naturally rare cell population and considering that we performed whole embryo single cell extraction from both embryonic and extra-embryonic compartments.

Quantification and Statistical Analysis

Statistical analysis was performed using the GraphPad Prism 8 software (La Joya, California). Data on graphs indicates means plus s.e.m. of a minimum of three independent experiments, unless otherwise stated. Kolmogorov-Smirnov test was performed to check normal distribution of data before each statistical

test. Significant difference between two samples was evaluated by One-Way ANOVA or unpaired two-sided Student's t-test if data was normally distributed or Mann-Whitney test for non-normally distributed data. $p < 0.05$ was considered as statistically significant.

Supplementary Video Legends

Supplementary Video S1. Advanced mouse synthetic embryos grown in electronically controlled ex utero platform and conditions (Related to Figure 2)

Electronically regulated roller culture incubator with customized gas concentration and pressure regulation module was utilized for growing mouse synthetic embryos as shown. Rotating glass bottles showing advanced mouse synthetic embryos (iCdx2 sEmbryos) at day 8 of ex utero culture protocol for synthetic embryos (as shown in **Figure 2D**).

Supplementary Video S2. E8.5 equivalent post-gastrulation synthetic mouse embryos (Related to Figure 2)

Part 1- Representative example of an undissected Day 8 synthetic embryo (iCdx2) within its extraembryonic compartments. Day 8 synthetic embryo (iCdx2) is showing beating heart, neural folds, allantois, vitelline circulation and ectoplacental cone. Part 2- Representative examples of dissected day 8 synthetic embryos after removal of extraembryonic tissues. Dissected Day 8 synthetic embryos are showing a beating heart, the neural tube and neural folds. Part 3 - Representative example of an undissected Day 8 synthetic embryo (eTSC) highlighting blood islands in yolk-sac and the ectoplacental cone. Day 8 synthetic embryo (eTSC) is showing vitelline circulation, blood islets formation in yolk-sac, a beating heart and an ectoplacental cone.

Supplementary Video S3. Mouse sEmbryos generated solely from naïve ESCs ex utero (Related to Figure 2)

Representative video captions showing different steps in generating sEmbryos until day 5 of the protocol (before the sEmbryos are transferred to the electronically controlled ex utero roller culture platform).

Supplementary Video S4. Setting up electronically controlled ex utero roller culture platform to grow post-gastrulation sEmbryos (Related to Figure 2)

Representative video captions showing different steps in setting up the electronically controlled ex utero roller culture platform in preparation for transferring naïve ESC derived day 5 sEmbryos.

Supplementary Video S5. Handling of sEmbryos grown in electronically controlled ex utero

roller culture platform (Related to Figure 2)

Representative video captions showing different steps in transferring and handling sEmbryos grown in electronically controlled ex utero roller culture platform from day 5 to 8.

Supplementary Spreadsheet Legends

Supplementary Spreadsheet 1: RNA-seq sample information and selected normalized expression patterns. (Related to Figures 1 and 7)

Sample information of 10X platform based single-cell RNA-seq samples. Sample information of bulk 3'UTR RNA-seq samples. Normalized expression values measured by bulk 3'UTR RNA-seq during induction of ESCs towards trophectoderm lineage and TSCs (eTSCs).

Supplementary Spreadsheet 2 – Sequence of PCR primers used in this study. (Related to STAR Methods)

References

Aguilera-Castrejon, A., Oldak, B., Shani, T., Ghanem, N., Itzkovich, C., Slomovich, S., Tarazi, S., Bayerl, J., Chugaeva, V., Ayyash, M., et al. (2021). Ex utero mouse embryogenesis from pre-gastrulation to late organogenesis. Nature *593*, 119–124. https://doi.org/10.1038/s41586-021-03416-3

Amadei, G., Lau, K.Y.C., de Jonghe, J., Gantner, C.W., Sozen, B., Chan, C., Zhu, M., Kyprianou, C., Hollfelder, F., and Zernicka-Goetz, M. (2021). Inducible Stem-Cell-Derived Embryos Capture Mouse Morphogenetic Events In Vitro. Developmental Cell *56*, 366-382.e9. https://doi.org/10.1016/j.devcel.2020.12.004

Anderson, K.G. v, Hamilton, W.B., Roske, F. v, Azad, A., Knudsen, T.E., Canham, M.A., Forrester, L.M., and Brickman, J.M. (2017). Insulin fine-tunes self-renewal pathways governing naive pluripotency and extra-embryonic endoderm. Nature Cell Biology *19*, 1164–1177. https://doi.org/10.1038/ncb3617

Bayerl J, Ayyash, M., Shani, T., Manor, Y., Gafni, O., Massarwa, R., Kalma, Y., Aguilera-Castrejon, A., Zerbib, M., Amir, H., et al. (2021). Principles of Signaling Pathway Modulation for Enhancing Human Naïve Pluripotency Induction. Cell Stem Cell *28, 1549-1565*. https://doi.org/10.1016/j.stem.2021.04.001

Beccari, L., Moris, N., Girgin, M., Turner, D.A., Baillie-Johnson, P., Cossy, A.-C., Lutolf, M.P., Duboule, D., and Arias, A.M. (2018). Multi-axial self-organization properties of mouse embryonic stem cells into gastruloids. Nature 562, 272-276. https://doi.org/10.1038/s41586-018-0578-0

Bedzhov, I., and Zernicka-Goetz, M. (2014). Self-Organizing Properties of Mouse Pluripotent Cells Initiate Morphogenesis upon Implantation. Cell 156, 1032-44. https://doi.org/10.1016/j.cell.2014.01.023

Benchetrit, H., Jaber, M., Zayat, V., Sebban, S., Pushett, A., Makedonski, K., Zakheim, Z., Radwan, A., Maoz, N., Lasry, R., et al. (2019). Direct Induction of the Three Pre-implantation Blastocyst Cell Types from Fibroblasts. Cell Stem Cell *24*, 983-994.e7. https://doi.org/10.1016/J.STEM.2019.03.018.

Blij, S., Parenti, A., Tabatabai-Yazdi, N., and Ralston, A. (2015). Cdx2 Efficiently Induces Trophoblast Stem-Like Cells in Naive, but Not Primed, Pluripotent Stem Cells. Stem Cells and Development 24, 1352-65. https://doi.org/10.1089/scd.2014.0395

Bradley, A., Evans, M., Kaufman, M.H., and Robertson, E. (1984) Formation of germ-line chimaeras from embryo-derived teratocarcinoma cell lines. Nature *309*, 255–256. https://doi.org/10.1038/309255a0

Cambuli, F., Murray, A., Dean, W., Dudzinska, D., Krueger, F., Andrews, S., Senner, C.E., Cook, S.J., and Hemberger, M. (2014). Epigenetic memory of the first cell fate decision prevents complete ES cell reprogramming into trophoblast. Nature Communications 5, *5538*. https://doi.org/10.1038/ncomms6538

Chan, M.M., Smith, Z.D., Grosswendt, S., Kretzmer, H., Norman, M., Adamson, B., Jost, M., Quinn, J.J., Yang, D., Jones, M.G., et al. (2019) Molecular recording of mammalian embryogenesis. Nature 570, 77-82. https://doi.org/10.1038/s41586-019-1184-5

Choi, J., Huebner, A.J., Clement, K., Walsh, R.M., Savol, A., Lin, K., Gu, H., di Stefano, B., Brumbaugh, J., Kim, S.Y., et al. (2017). Prolonged Mek1/2 suppression impairs the developmental potential of embryonic stem cells. Nature *548*, 219–223. https://doi.org/10.1038/nature23274

Fujikura, J., Yamato, E., Yonemura, S., Hosoda, K., Masui, S., Nakao, K., Miyazaki Ji, J., and Niwa, H. (2002). Differentiation of embryonic stem cells is induced by GATA factors. Genes Dev *16*, 784–789. https://doi.org/10.1101/gad.968802

Gafni, O., Weinberger, L., Mansour, A.A., Manor, Y.S., Chomsky, E., Ben-Yosef, D., Kalma, Y., Viukov, S., Maza, I., Zviran, A., et al. (2013). Derivation of novel human ground state naive pluripotent stem cells. Nature *504*, 282–286. https://doi.org/10.1038/nature12745.

Hanna, J., Markoulaki, S., Mitalipova, M., Cheng, A.W., Cassady, J.P., Staerk, J., Carey, B.W., Lengner, C.J., Foreman, R., Love, J., et al. (2009). Metastable pluripotent states in NOD-mouse-derived ESCs. Cell Stem Cell *4*, 513–524. https://doi.org/10.1016/j.stem.2009.04.015

Harrison, S.E., Sozen, B., Christodoulou, N., Kyprianou, C., and Zernicka-Goetz, M. (2017). Assembly of embryonic and extraembryonic stem cells to mimic embryogenesis in vitro. Science *356 (6334)*. https://doi.org/10.1126/science.aal1810

Hayashi, K., Ohta, H., Kurimoto, K., Aramaki, S., and Saitou, M. (2011). Reconstitution of the mouse germ cell specification pathway in culture by pluripotent stem cells. Cell *146*, 519–532. https://doi.org/10.1016/j.cell.2011.06.052

Hochedlinger, K., Yamada, Y., Beard, C., and Jaenisch, R. (2005). Ectopic expression of Oct-4 blocks progenitor-cell differentiation and causes dysplasia in epithelial tissues. Cell *121*, 465–477. https://doi.org/10.1016/j.cell.2005.02.018

Ibarra-Soria, X., Jawaid, W., Pijuan-Sala, B., Ladopoulos, V., Scialdone, A., Jörg, D.J., Tyser, R.C.V., Calero-Nieto, F.J., Mulas, C., Nichols, J., et al. (2018). Defining murine organogenesis at single-cell resolution reveals a role for the leukotriene pathway in regulating blood progenitor formation. Nature Cell Biology *20*, 127–134. https://doi.org/10.1038/s41556-017-0013-z

Iturri, L., Freyer, L., Biton, A., Dardenne, P., Lallemand, Y., and Gomez Perdiguero, E. (2021). Megakaryocyte production is sustained by direct differentiation from erythromyeloid progenitors in the yolk sac until midgestation. Immunity *54*, 1433-1446. https://doi.org/10.1016/j.immuni.2021.04.026

Kagawa, H., Javali, A., Khoei, H.H., Sommer, T.M., Sestini, G., Novatchkova, M., Scholte Op Reimer, Y., Castel, G., Bruneau, A., Maenhoudt, N., et al. (2022). Human blastoids model blastocyst development and implantation. Nature *601*, 600-605. https://doi.org/10.1038/s41586-021-04267-8

Keren-Shaul, H., Kenigsberg, E., Jaitin, D.A., David, E., Paul, F., Tanay, A., and Amit, I. (2019) MARS-seq2.0: an experimental and analytical pipeline for indexed sorting combined with single-cell RNA sequencing. Nature Protocols 14, 1841-1862. https://doi.org/10.1038/s41596-019-0164-4

Kunath, T., Arnaud, D., Uy, G.D., Okamoto, I., Chureau, C., Yamanaka, Y., Heard, E., Gardner, R.L., Avner, P., and Rossant, J. (2005). Imprinted X-inactivation in extra-embryonic endoderm cell lines from mouse blastocysts. Development *132*, 1649–1661. https://doi.org/10.1242/dev.01715

Lancaster, M.A., Renner, M., Martin, C.-A., Wenzel, D., Bicknell, L.S., Hurles, M.E., Homfray, T., Penninger, J.M., Jackson, A.P., and Knoblich, J.A. (2013). Cerebral organoids model human brain development and microcephaly. Nature 501, 373-379. https://doi.org/10.1038/nature12517

Lee, C.Q.E., Gardner, L., Turco, M., Zhao, N., Murray, M.J., Coleman, N., Rossant, J., Hemberger, M., and Moffett, A. (2016). What Is Trophoblast? A Combination of Criteria Define Human First-Trimester Trophoblast. Stem Cell Reports *6*, 1–16. https://doi.org/10.1016/j.stemcr.2016.01.006

van Maele-Fabry, G., Delhaise, F., and Picard, J.J. (1992). Evolution of the developmental scores of sixteen morphological features in mouse embryos displaying 0 to 30 somites. International Journal of Developmental Biology *36*, 161–167.

Mandrycky, C.J., Williams, N.P., Batalov, I., El-Nachef, D., de Bakker, B.S., Davis, J., Kim, D.H., DeForest, C.A., Zheng, Y., Stevens, K.R., et al. (2020). Engineering Heart Morphogenesis. Trends in Biotechnology *38*, 835–845. https://doi.org/10.1016/j.tibtech.2020.01.006

Mittenzweig, M., Mayshar, Y., Ben-Yair, R., Hadas, R., Rais, Y., Chomsky, E., Reines, N., Uzonyi, A., Lumerman, L., Lifshitz, A., et al. (2021). A single embryo, single cell time-resolved model for mouse gastrulation. Cell *184*, 2825-2842. https://doi.org/10.1016/j.cell.2021.04.004

Morgani, S.M., Canham, M.A., Nichols, J., Sharov, A.A., Migueles, R.P., Ko, M.S.H., and Brickman, J.M. (2013). Totipotent Embryonic Stem Cells Arise in Ground-State Culture Conditions. Cell Reports *3*, 1945–1957. https://doi.org/10.1016/j.celrep.2013.04.034

New, D.A.T. (1978). Whole embryo culture and the study of mammalian embryos during organogenesis. Biological Reviews *53*, 81–122. https://doi.org/10.1111/j.1469-185x.1978.tb00993.x

Nichols, J., and Smith, A. (2009). Naive and Primed Pluripotent States. Cell Stem Cell *4*, 487–492. https://doi.org/10.1016/j.stem.2009.05.015

Niwa, H., Toyooka, Y., Shimosato, D., Strumpf, D., Takahashi, K., Yagi, R., and Rossant, J. (2005). Interaction between Oct3/4 and Cdx2 determines trophectoderm differentiation. Cell *123*, 917–929. https://doi.org/10.1016/j.cell.2005.08.040

Parameswaran, M., and Tam, P.P.L. (1995). Regionalisation of cell fate and morphogenetic movement of the mesoderm during mouse gastrulation. Developmental Genetics *17*, 16–28. https://doi.org/10.1002/dvg.1020170104

Rivron, N.C., Frias-Aldeguer, J., Vrij, E.J., Boisset, J.C., Korving, J., Vivié, J., Truckenmüller, R.K., van Oudenaarden, A., van Blitterswijk, C.A., and Geijsen, N. (2018). Blastocyst-like structures generated solely from stem cells. Nature *557*, 106–111. https://doi.org/10.1038/s41586-018-0051-0

Seong, J., Frias-Aldeguer, J., Holzmann, V., Kagawa, H., Sestini, G., Heidari Khoei, H., Scholte Op Reimer, Y., Kip, M., Pradhan, S.J., Verwegen, L., et al. (2022). Epiblast inducers capture mouse trophectoderm stem cells in vitro and pattern blastoids for implantation in utero. Cell Stem Cell *29*, 1102-1118.e8. https://doi.org/10.1016/j.stem.2022.06.002

Shimizu, T., Ueda, J., Ho, J.C., Iwasaki, K., Poellinger, L., Harada, I., and Sawada, Y. (2012). Dual Inhibition of Src and GSK3 Maintains Mouse Embryonic Stem Cells, Whose Differentiation Is Mechanically Regulated by Src Signaling. Stem Cells *30*, 1394–1404. https://doi.org/10.1002/stem.1119

Sozen, B., Amadei, G., Cox, A., Wang, R., Na, E., Czukiewska, S., Chappell, L., Voet, T., Michel, G., Jing, N., et al. (2018). Self-assembly of embryonic and two extra-embryonic stem cell types into gastrulating embryo-like structures. Nature Cell Biology *20*, 979–989. https://doi.org/10.1038/s41556-018-0147-7

Tam, P.P. (1998). Postimplantation mouse development: whole embryo culture and micro-manipulation. The International Journal of Developmental Biology *42*, 895–902.

Tam, P.P.L., and Snow, M.H.L. (1980). The in vitro culture of primitive-streak-stage mouse embryos. J. Embryol. Exp. Morphol. 59,131-43.

Tanaka, S., Kunath, T., Hadjantonakis, A.K., Nagy, A., and Rossant, J. (1998). Promotion of trophoblast stem cell proliferation by FGF4. Science *282*, 2072–2075. https://doi.org/10.1126/science.282.5396.2072

Veenvliet, J. v., Bolondi, A., Kretzmer, H., Haut, L., Scholze-Wittler, M., Schifferl, D., Koch, F., Guignard, L., Kumar, A.S., Pustet, M., et al. (2020). Mouse embryonic stem cells self-organize into trunk-like structures with neural tube and somites. Science *370* (6522). https://doi.org/10.1126/science.aba4937

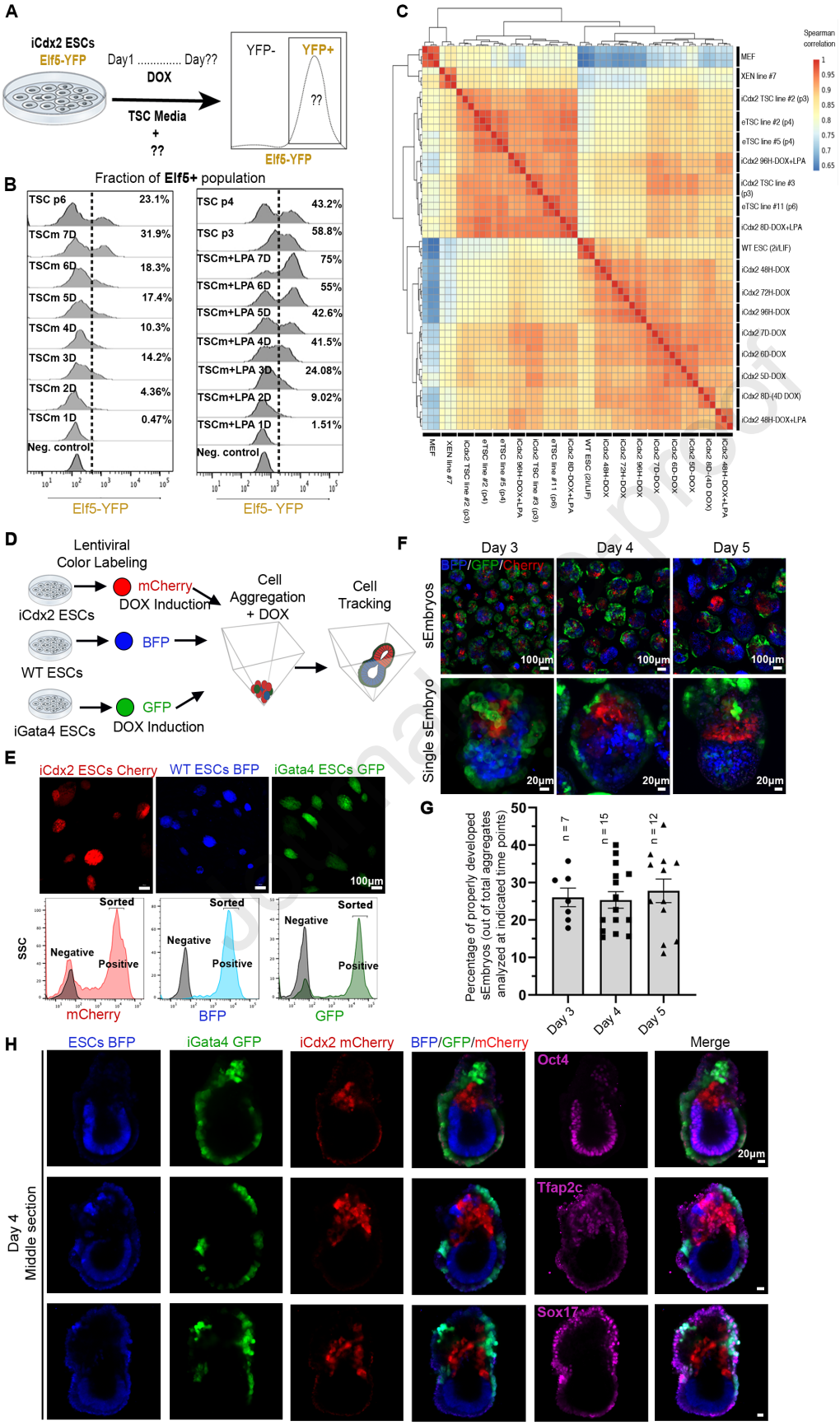
A
iCdx2 ESCs
Elf5-YFP
Day1 ..... Day??
DOX
TSC Media
+
??
YFP-
YFP+
??
Elf5-YFP
B
Fraction of Elf5+ population
TSC p6 23.1%
TSCm 7D 31.9%
TSCm 6D 18.3%
TSCm 5D 17.4%
TSCm 4D 10.3%
TSCm 3D 14.2%
TSCm 2D 4.36%
TSCm 1D 0.47%
Neg. control
Elf5-YFP
TSC p4 43.2%
TSC p3 58.8%
TSCm+LPA 7D 75%
TSCm+LPA 6D 55%
TSCm+LPA 5D 42.6%
TSCm+LPA 4D 41.5%
TSCm+LPA 3D 24.08%
TSCm+LPA 2D 9.02%
TSCm+LPA 1D 1.51%
Neg. control
Elf5- YFP
C
Spearman correlation
1
0.95
0.9
0.85
0.8
0.75
0.7
0.65
MEF
XEN line #7
iCdx2 TSC line #2 (p3)
eTSC line #2 (p4)
eTSC line #5 (p4)
iCdx2 96H-DOX+LPA
iCdx2 TSC line #3 (p3)
eTSC line #11 (p6)
iCdx2 8D-DOX+LPA
WT ESC (2i/LIF)
iCdx2 48H-DOX
iCdx2 72H-DOX
iCdx2 96H-DOX
iCdx2 7D-DOX
iCdx2 6D-DOX
iCdx2 5D-DOX
iCdx2 8D-(4D DOX)
iCdx2 48H-DOX+LPA
D
Lentiviral
Color Labeling
iCdx2 ESCs
mCherry
DOX Induction
WT ESCs
BFP
iGata4 ESCs
GFP
DOX Induction
Cell
Aggregation
+ DOX
Cell
Tracking
E
iCdx2 ESCs Cherry
WT ESCs BFP
iGata4 ESCs GFP
100μm
SSC
Sorted
Negative
Positive
mCherry
BFP
GFP
F
Day 3
Day 4
Day 5
sEmbryos
Single sEmbryo
BFP/GFP/Cherry
100μm
20μm
G
Percentage of properly developed sEmbryos (out of total aggregates analyzed at indicated time points)
n = 7
n = 15
n = 12
Day 3
Day 4
Day 5
H
ESCs BFP
iGata4 GFP
iCdx2 mCherry
BFP/GFP/mCherry
Merge
Oct4
Tfap2c
Sox17
Day 4
Middle section
20μm

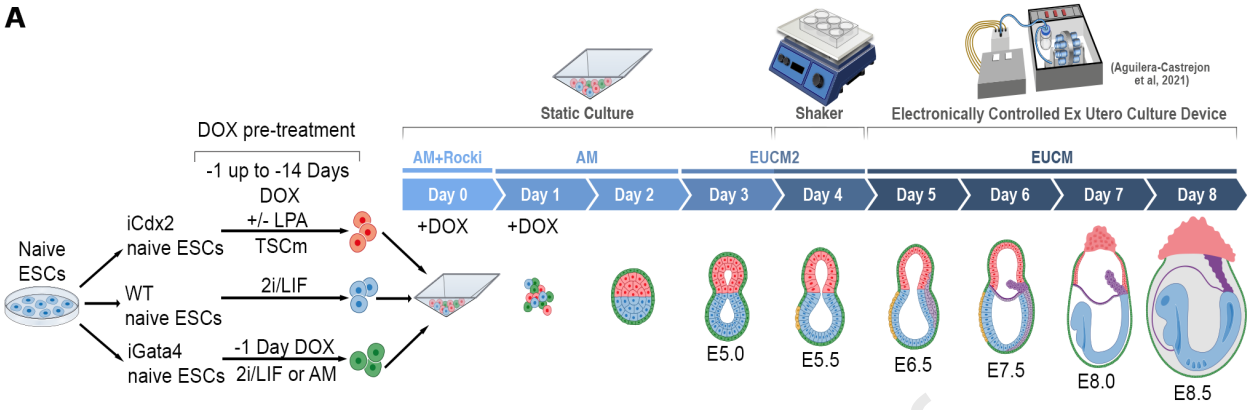
A
Static Culture
Shaker
(Aguilera-Castrejon et al, 2021)
Electronically Controlled Ex Utero Culture Device
DOX pre-treatment
-1 up to -14 Days DOX
AM+Rocki
AM
EUCM2
EUCM
Day 0
Day 1
Day 2
Day 3
Day 4
Day 5
Day 6
Day 7
Day 8
+DOX
+DOX
Naive ESCs
iCdx2 naive ESCs
+/- LPA
TSCm
WT naive ESCs
2i/LIF
iGata4 naive ESCs
-1 Day DOX
2i/LIF or AM
E5.0
E5.5
E6.5
E7.5
E8.0
E8.5

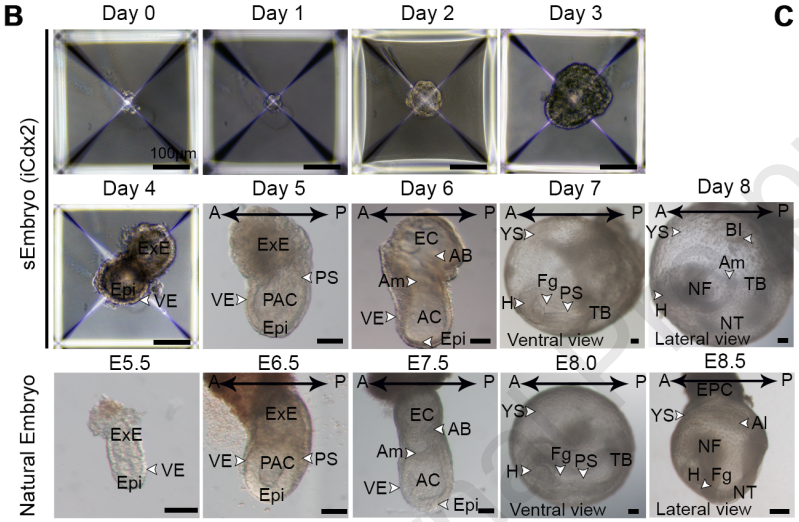
B
Day 0
Day 1
Day 2
Day 3
sEmbryo (iCdx2)
100µm
Day 4
Day 5
Day 6
Day 7
Day 8
ExE
Epi
VE
PAC
PS
EC
AB
Am
AC
YS
Fg
TB
H
NF
NT
BI
Ventral view
Lateral view
Natural Embryo
E5.5
E6.5
E7.5
E8.0
E8.5
EPC
Al

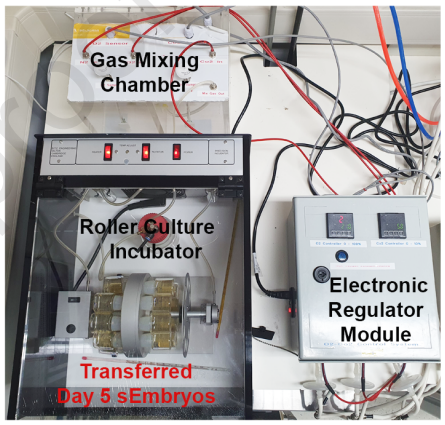
C
Gas Mixing Chamber
Roller Culture Incubator
Electronic Regulator Module
Transferred Day 5 sEmbryos

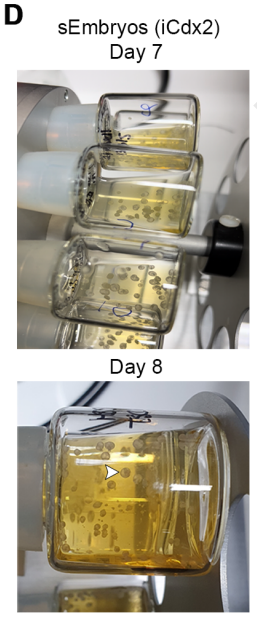
D
sEmbryos (iCdx2)
Day 7
Day 8

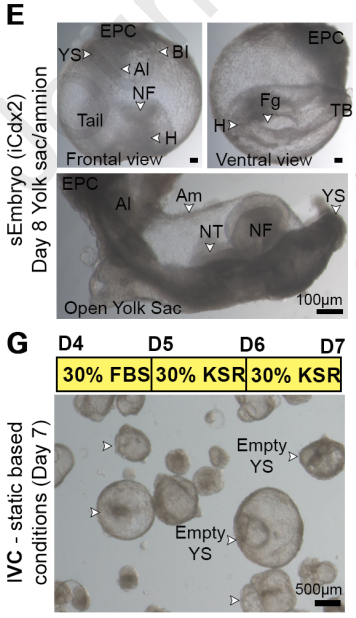
E
sEmbryo (iCdx2) Day 8 Yolk sac/amnion
EPC
YS
BI
Al
NF
Tail
H
Frontal view
Fg
TB
Ventral view
Am
NT
Open Yolk Sac
100µm
G
D4
D5
D6
D7
30% FBS
30% KSR
30% KSR
IVC - static based conditions (Day 7)
Empty YS
500µm

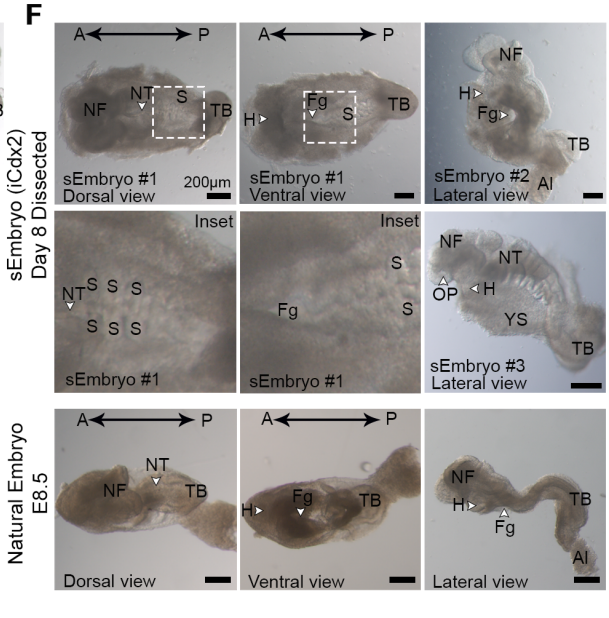
F
sEmbryo (iCdx2) Day 8 Dissected
A
P
NF
NT
S
TB
H
Fg
sEmbryo #1
Dorsal view
200µm
Ventral view
sEmbryo #2
Lateral view
Al
Inset
OP
YS
sEmbryo #3
Natural Embryo E8.5
Dorsal view
Ventral view
Lateral view

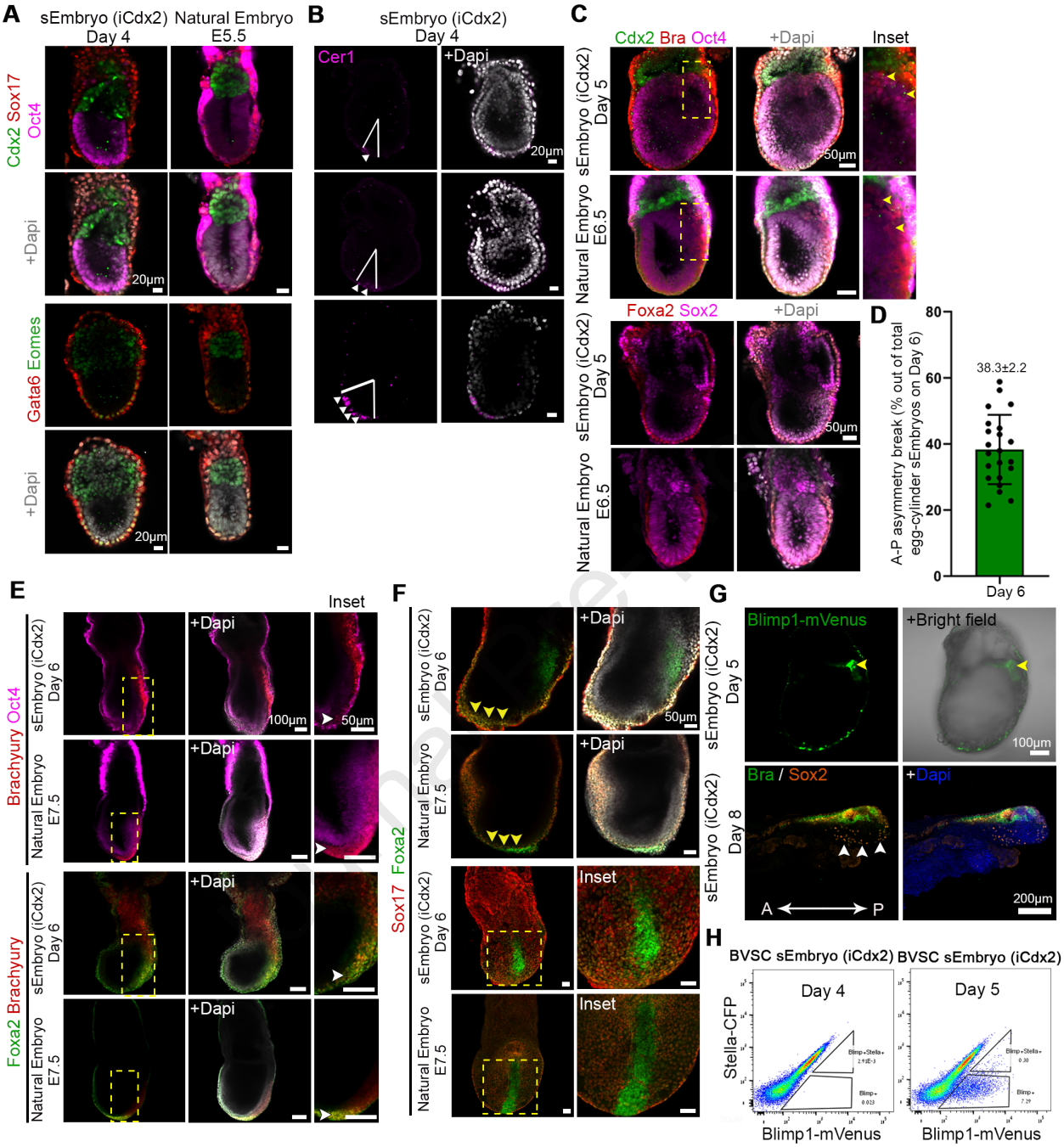
A
sEmbryo (iCdx2) Day 4
Natural Embryo E5.5
Cdx2 Sox17 Oct4
+Dapi
Gata6 Eomes
+Dapi
20μm
B
sEmbryo (iCdx2) Day 4
Cer1
+Dapi
20μm
C
Cdx2 Bra Oct4
+Dapi
Inset
sEmbryo (iCdx2) Day 5
Natural Embryo E6.5
50μm
Foxa2 Sox2
+Dapi
D
A-P asymmetry break (% out of total egg-cylinder sEmbryos on Day 6)
38.3±2.2
Day 6
E
Inset
Brachyury Oct4
sEmbryo (iCdx2) Day 6
Natural Embryo E7.5
+Dapi
100μm
50μm
Foxa2 Brachyury
F
Sox17 Foxa2
Inset
G
Blimp1-mVenus
+Bright field
100μm
Bra / Sox2
A
P
200μm
H
BVSC sEmbryo (iCdx2)
Day 4
Day 5
Stella-CFP
Blimp1-mVenus

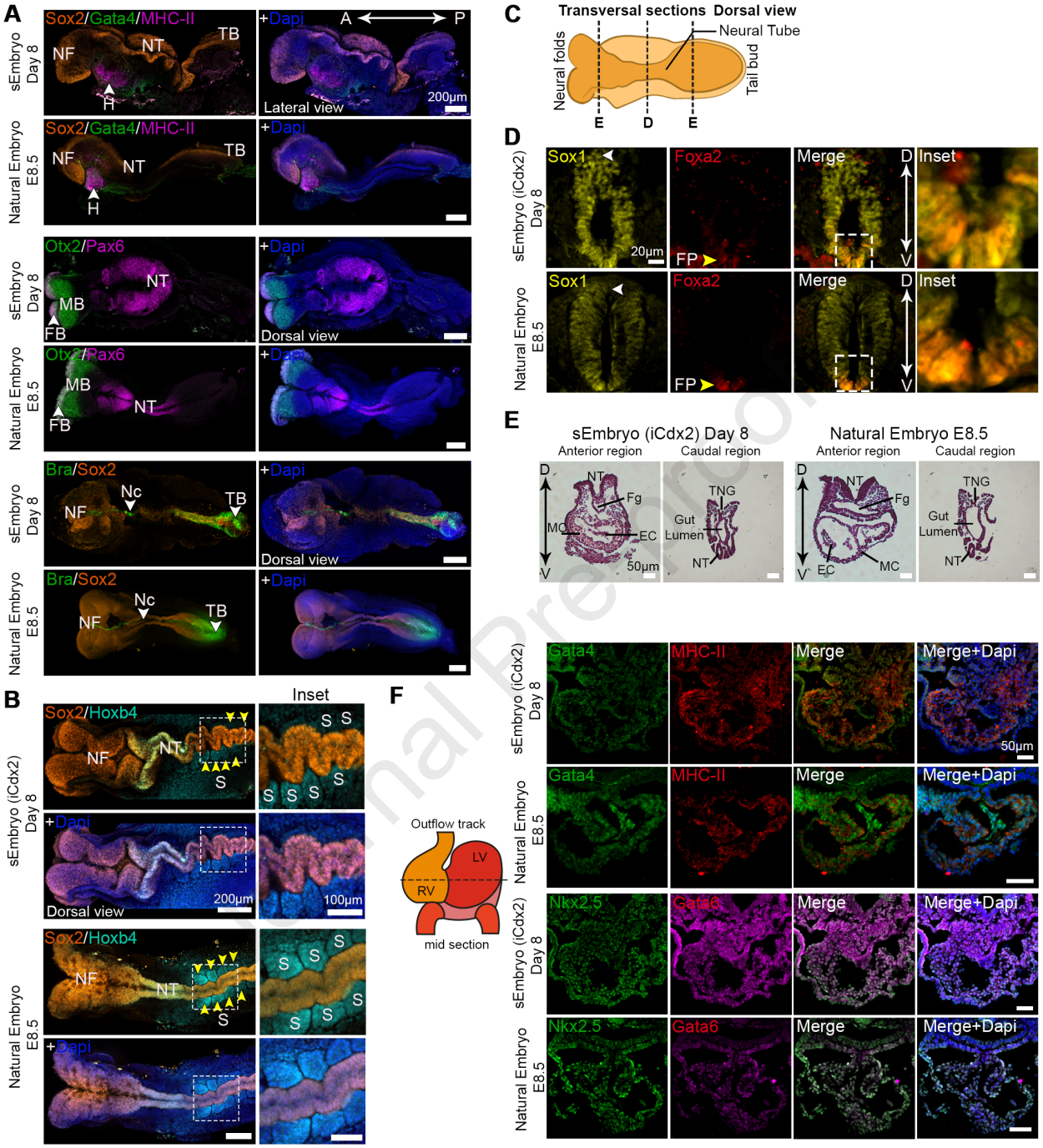
A
Sox2/Gata4/MHC-II
+Dapi
sEmbryo Day 8
Natural Embryo E8.5
NF
NT
TB
H
A
P
Lateral view
200µm
Otx2/Pax6
MB
FB
Dorsal view
Bra/Sox2
Nc
B
Sox2/Hoxb4
Inset
S
200µm
100µm
sEmbryo (iCdx2) Day 8
C
Transversal sections
Dorsal view
Neural Tube
Neural folds
Tail bud
E
D
Sox1
Foxa2
Merge
Inset
FP
20µm
D
V
E
sEmbryo (iCdx2) Day 8
Natural Embryo E8.5
Anterior region
Caudal region
Fg
MC
EC
TNG
Gut Lumen
50µm
F
Outflow track
LV
RV
mid section
Gata4
MHC-II
Merge
Merge+Dapi
Nkx2.5
Gata6

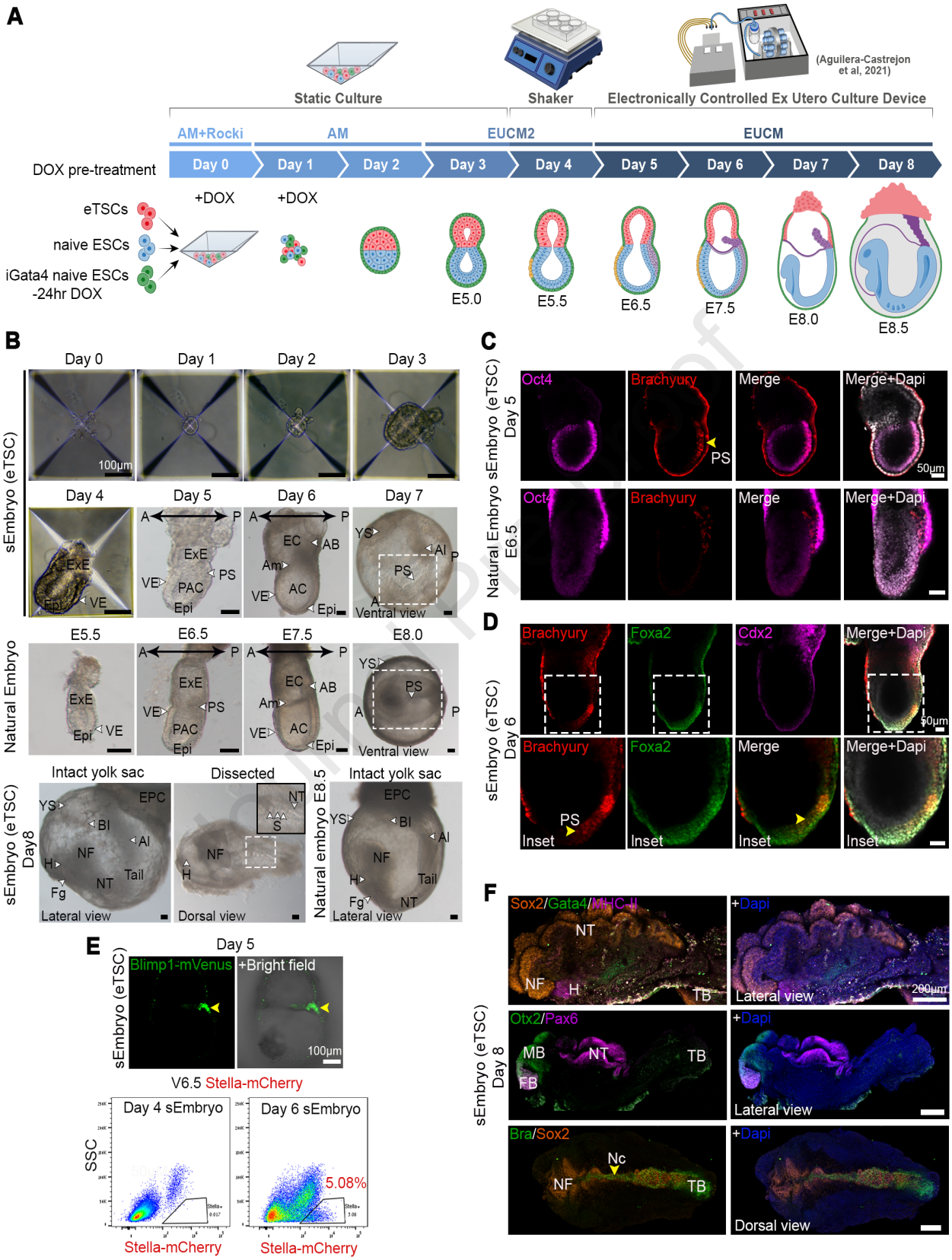
A
Static Culture
Shaker
(Aguilera-Castrejon et al, 2021)
Electronically Controlled Ex Utero Culture Device
AM+Rocki
AM
EUCM2
EUCM
DOX pre-treatment
Day 0
Day 1
Day 2
Day 3
Day 4
Day 5
Day 6
Day 7
Day 8
+DOX
+DOX
eTSCs
naive ESCs
iGata4 naive ESCs
-24hr DOX
E5.0
E5.5
E6.5
E7.5
E8.0
E8.5
B
Day 0
Day 1
Day 2
Day 3
sEmbryo (eTSC)
100μm
Day 4
Day 5
Day 6
Day 7
ExE
Epi
VE
PS
PAC
EC
AB
Am
AC
YS
Al
Ventral view
Natural Embryo
E5.5
E6.5
E7.5
E8.0
Intact yolk sac
Dissected
Intact yolk sac
sEmbryo (eTSC) Day8
Natural embryo E8.5
EPC
BI
NF
H
Tail
NT
Fg
S
Lateral view
Dorsal view
C
Natural Embryo sEmbryo (eTSC) Day 5
Natural Embryo E6.5
Oct4
Brachyury
Merge
Merge+Dapi
PS
50μm
D
sEmbryo (eTSC) Day 6
Foxa2
Cdx2
Inset
E
Day 5
sEmbryo (eTSC)
Blimp1-mVenus
+Bright field
100μm
V6.5 Stella-mCherry
Day 4 sEmbryo
Day 6 sEmbryo
SSC
5.08%
Stella-mCherry
F
sEmbryo (eTSC) Day 8
Sox2/Gata4/MHC-II
+Dapi
TB
200μm
Otx2/Pax6
MB
FB
Bra/Sox2
Nc

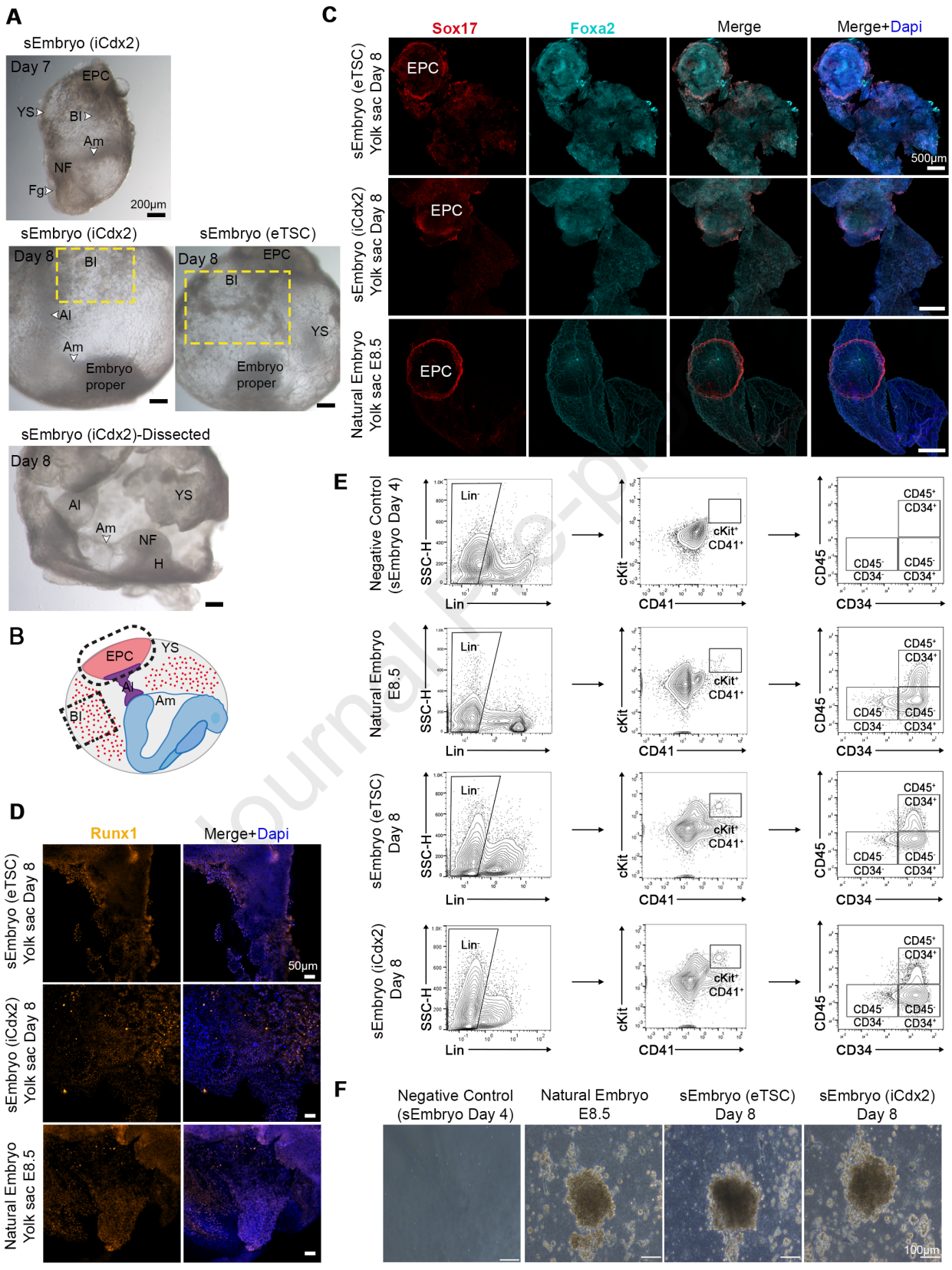
A
sEmbryo (iCdx2)
Day 7
EPC
YS
Bl
Am
NF
Fg
200μm
sEmbryo (iCdx2)
Day 8
Bl
Al
Am
Embryo proper
sEmbryo (eTSC)
Day 8
EPC
Bl
YS
Embryo proper
sEmbryo (iCdx2)-Dissected
Day 8
Al
YS
Am
NF
H
B
EPC
YS
Al
Am
Bl
C
Sox17
Foxa2
Merge
Merge+Dapi
sEmbryo (eTSC) Yolk sac Day 8
sEmbryo (iCdx2) Yolk sac Day 8
Natural Embryo Yolk sac E8.5
EPC
500μm
D
Runx1
Merge+Dapi
sEmbryo (eTSC) Yolk sac Day 8
sEmbryo (iCdx2) Yolk sac Day 8
Natural Embryo Yolk sac E8.5
50μm
E
Negative Control (sEmbryo Day 4)
Natural Embryo E8.5
sEmbryo (eTSC) Day 8
sEmbryo (iCdx2) Day 8
SSC-H
Lin
cKit
CD41
CD45
CD34
Lin⁻
cKit⁺ CD41⁺
CD45⁺ CD34⁺
CD45⁻ CD34⁻
CD45⁻ CD34⁺
F
Negative Control (sEmbryo Day 4)
Natural Embryo E8.5
sEmbryo (eTSC) Day 8
sEmbryo (iCdx2) Day 8
100μm

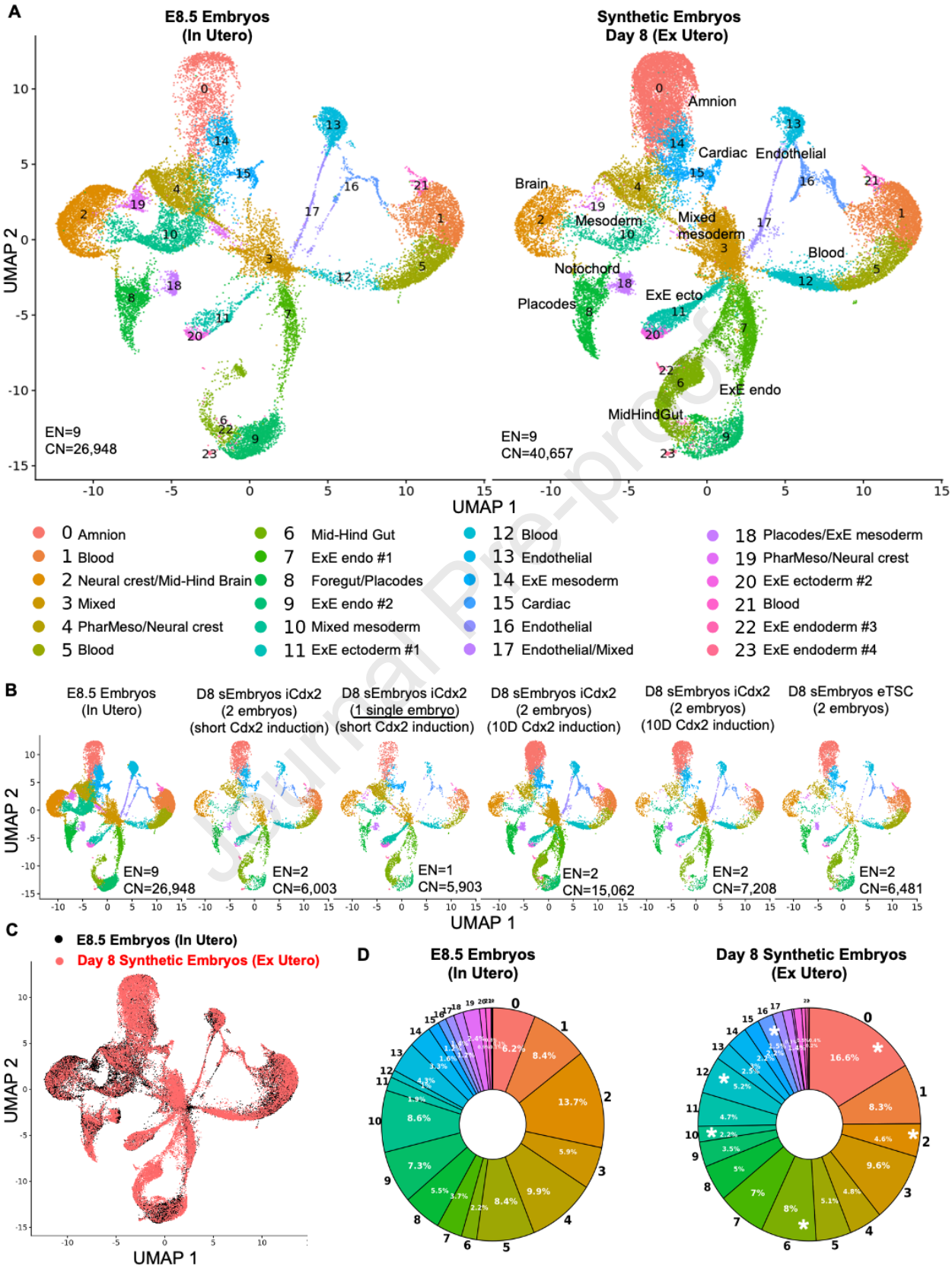

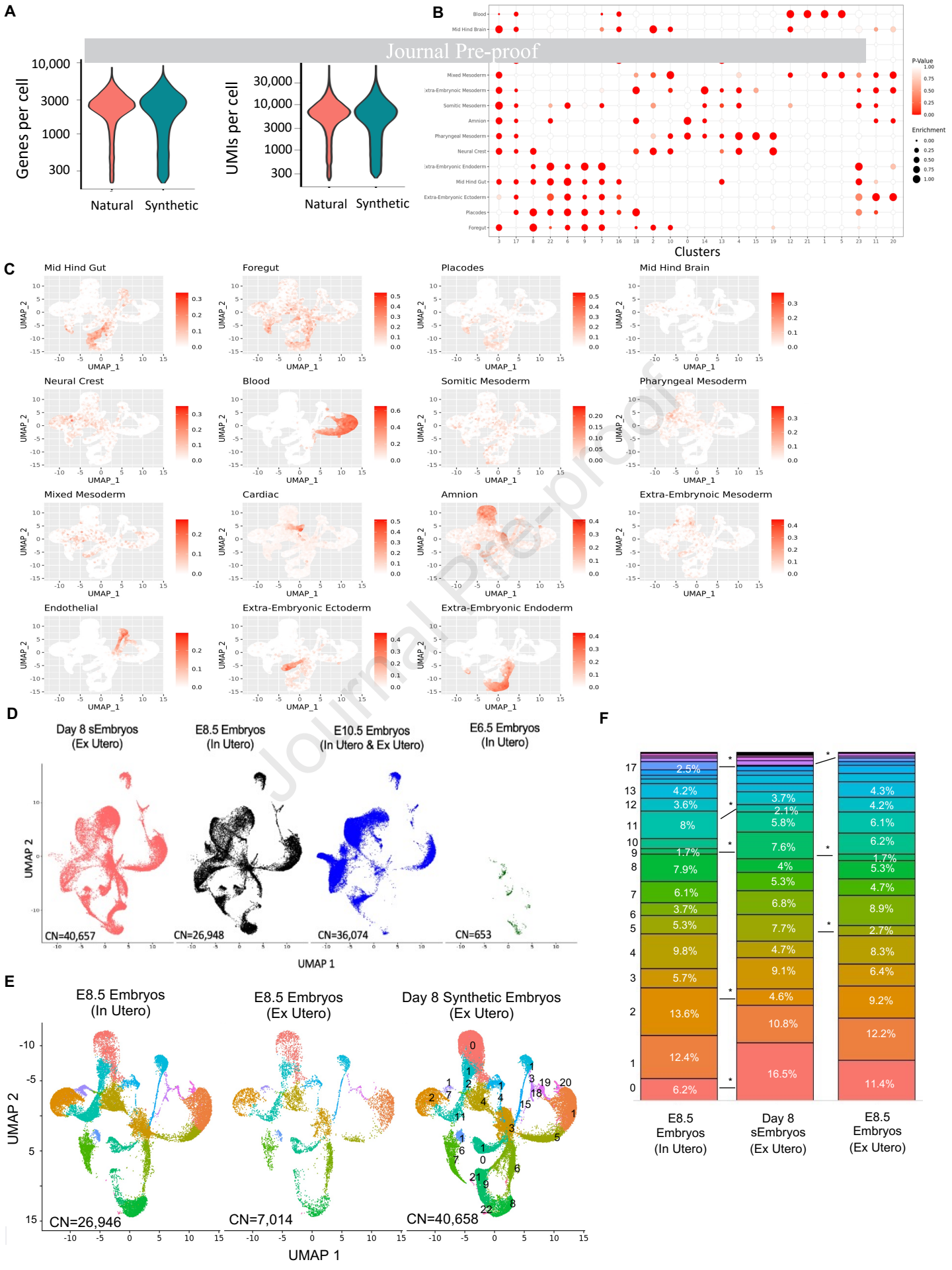

Highlights

- Advanced synthetic embryos (sEmbryos) self-assembled from ESCs in an ex utero setup
- Naïve ESCs give rise to all embryonic and extra-embryonic compartments in sEmbryos
- Post-gastrulation stem cell derived sEmbryos develop organ specific progenitors
- Extra-embryonic compartments adequately develop in post-gastrulation whole sEmbryos

eToc/In brief:

Post-gastrulation stages of development with organ progenitors and complex extra-embryonic compartments are achieved entirely from assembled naïve mouse embryonic stem cells

Key resources table

REAGENT or RESOURCE	SOURCE	IDENTIFIER
Antibodies		
Rabbit anti-Gata4 (1:200)	Abcam	Cat# Ab84593; RRID: AB_10670538
Rabbit anti-Foxa2 (1:100)	Abcam	Cat# Ab40874; RRID: AB_732411
Goat anti-Sox2 (1:200)	R&D	Cat# AF2018; RRID: AB_355110
Mouse Anti-Myosin Heavy Chain 2 (1:100)	R&D	Cat# MAB4470; Clone# MF-20; RRID: AB_1293549
Goat anti-Sox17 (1:100)	R&D	Cat# AF1924; RRID: AB_355060
Rabbit anti-Brachyury (1:100)	Cell Signaling	Cat# 81694; RRID: AB_2799983
Rabbit anti-Cdx2 (1:100)	Abcam	Cat# Ab76541; RRID: AB_1523334
Mouse anti-Oct3/4 (1:100)	Santa Cruz	Cat# Sc-5279; RRID: AB_628051
Goat anti-Otx2 (1:100)	R&D	Cat# AF1979; RRID: AB_2157172
Goat anti-Tfap2c/Ap2γ (1:100)	R&D	Cat# AF5059; RRID: AB_2255891
Goat anti-Gata6 (1:100)	R&D	Cat# AF1700; RRID: AB_2108901
Rabbit anti-Eomes/Tbr2 (1:50)	Abcam	Cat# Ab23345; RRID: AB_778267
Rat anti-Cerberus 1 (1:100)	R&D	Cat# MAB1986; RRID: AB_2275974
Rabbit anti-Sox9 (1:100)	Millipore	Cat# Ab5535; RRID: AB_2239761
Mouse anti-Gata3 (1:100)	Invitrogen	Cat# MA1-028; RRID: AB_2536713
Rabbit anti-Nanog (1:100)	Bethyl	Cat# AF1997; RRID: AB_355097
Goat anti-Elf5 (1:100)	Santa Cruz	Cat# Sc-9645; RRID: AB_640106
Goat anti-Dkk1 (1:100)	R&D	Cat# AF1096; RRID: AB_354597
Goat anti-Brachyury (1:100)	R&D	Cat# AF2085; RRID: AB_2200235
Rabbit anti-Nkx2.5 (1:100)	Abcam	Cat# Ab97355; RRID: AB_10680260
Rabbit anti-Hoxb4 (1:100)	Abcam	Cat#: ab133521; Clone: ERP1917
Rabbit anti-Pax6 (1:100)	Biolegend	Cat#: 901301; RRID: AB_2565003
Rabbit anti-Runx1 (1:100)	Abcam	Cat#: ab240639; Clone: ERP23044-100
Rat anti-cKit (1:50)	Biolegend	Cat# 105802; RRID: AB_313211

Rat anti-CD45 (1:100)	Biolegend	Cat# 103102; RRID: AB_312967
Rat anti-CD41 (1:50)	Biolegend	Cat# 133906; RRID: AB_2129745
Rat anti-CD34 (1:50)	eBioscience	Cat# 14-0341-82; RRID: AB_467210
Streptavidin-PE-Cy7	Biolegend	Cat# 405206;
Mouse Lineage cell detection cocktail-biotin (1:20)	Miltenyi	Cat#130-092-613; RRID: AB_1103214
Alexa Fluor 488-conjugated AffiniPure Donkey anti-rabbit IgG (H+L)	Jackson	Cat# 711-545-152; RRID: AB_2313584
Alexa Fluor 488-conjugated AffiniPure Donkey anti-Goat IgG (H+L)	Jackson	Cat# 705-545-003; RRID: AB_2340428
Rhodamine-Red-X-conjugated AffiniPure Donkey anti-Rabbit IgG (H+L)	Jackson	Cat# 711-295-152; RRID: AB_2340613
Rhodamine-Red-X-conjugated AffiniPure Donkey anti-Gaot IgG (H+L)	Jackson	Cat# 705-295-003; RRID: AB_2340422
Rhodamine-Red-X-conjugated AffiniPure Donkey anti-Mouse IgG (H+L)	Jackson	Cat# 715-295-150; RRID: AB_2340831
Alexa Fluor 647-conjugated AffiniPure Donkey anti-rabbit IgG (H+L)	Jackson	Cat# 711-605-152; RRID: AB_2492288
Alexa Fluor 647-conjugated AffiniPure Donkey anti-Goat IgG (H+L)	Jackson	Cat# 705-605-003; RRID: AB_2340436
Alexa Fluor 647-conjugated AffiniPure Donkey anti-Mouse IgG (H+L)	Jackson	Cat# 715-605-150; RRID: AB_2340862
Alexa Fluor 647-conjugated AffiniPure Donkey anti-Rat IgG (H+L)	Jackson	Cat# 712-545-153; RRID: AB_2340684
Bacterial and virus strains		
Biological samples		
Chemicals, peptides, and recombinant proteins		
FGF4	Peprotech	100-31
Heparin	Sigma	H3149
0.25% Trypsin-EDTA	Biological industries-Sartorius	03-050-1B
0.05% trypsin-EDTA	Biological industries-Sartorius	03-053-1B
DMEM Medium	GIBCO	41965
FBS Serum (for growing MEFs and ES lines)	GIBCO	10270-106
GlutaMAX	GIBCO	35050061
Penicillin streptomycin	Biological industries-Sartorius	03-031-1B

Sodium Pyruvate	Biological industries-Sartorius	03-042-1B
Nonessential amino acids	Biological industries-Sartorius	01-340-1B
β-Mercaptoethanol	Thermo	31350010
Recombinant Human LIF	This study	N/A
Neurobasal	Thermo	21103049
DMEM-F12 with HEPES Medium	Sigma	D6421
N2	Invitrogen	17502048
B27	Invitrogen	17504044
CHIR99021	Axon Medchem	1386
PD0325901	Axon Medchem	1408
RPMI1640	GIBCO	21875
FBS (for sEmbryo aggregation stages)	Sigma	F7524
Doxycycline	Sigma	D9891
ROCKi Y27632	Axon Medchem	1683
LPA (Oleoyl-L-α-lysophosphatidic acid)	Sigma	L7260
Advanced DMEM/F12	GIBCO	21331-020
D(+)-Glucose Monohydrate	J.T. Baker	0113
T3 (3,3′,5-Triiodo-L-thyronine sodium salt)	Sigma-Aldrich	T6397
HEPES	GIBCO	15630056
CMRL	GIBCO	11530037
ITS-X	Thermo Fisher Scientific	51500-056
B-estradiol	Sigma	E8875
Progesterone	Sigma	P0130
N-acetyl-L-cysteine	Sigma	A7250
DMEM W/O phenol red W/O L-glutamine Medium	GIBCO	11880
Rat Serum	ENVIGO Bioproducts	B-4520
MethoCult	Stem Cell Technologies	SF M3436
Normal Donkey Serum	Jackson Laborratories	017-000-121
Critical commercial assays		
Syber Green PCR master Mix	Thermo Fisher	4385614
JetPEI Transfection Reagent	Polyplus Inc.	101-10N
Deposited data		
scRNA-seq data E8.5 natural ex Utero	Aguilera-Castrejon et al., 2021	GSE149372
scRNA-seq data	This study	GSE208681
Bulk MARS RNA- seq data	This study	GSE208681
Additional supplementary technical data and results	This study	Mendeley Data: doi 10.17632/6nhpgnxf3y.1
Experimental models: Cell lines		

Mouse: BVSC ESC (Blimp1-mVenus-Stella-CFP ESCs)	Hayashi et al., 2011	N/A
Mouse: V6.5 WT ESCs	Hochedlinger et al., 2005	N/A
Mouse: KH2 WT ESCs	Hochedlinger et al., 2005	N/A
Mouse: ICR1 ESCs	This study	N/A
Mouse: BDF2 TSCs (clone #2 and #5)	This study	N/A
Mouse: ICR XEN (clone #7)	This study	N/A
Mouse: KH2-Cdx2 ESCs (clone #3) (iCdx2)	This study	N/A
Mouse: KH2-Cdx2-Elf5-EYFP (clone #6)	This study	N/A
Mouse: KH2-Gata4 ESCs (clone #7) (iGata4)	This study	N/A
Human: HEK293T	ATCC	N/A
Experimental models: Organisms/strains		
Mouse: BDF1	ENVIGO	N/A
Mouse: 129sJae	ENVIGO	N/A
Mouse: ICR	ENVIGO	N/A
Oligonucleotides		
Supplementary Spreadsheet 2	This study	N/A
Recombinant DNA		
TetO-Cdx2 flip-in construct	This study	N/A
TetO-Gata4 flip-in construct	This study	N/A
Elf5-EYFP targeting vector	Benchetrit et al., 2019	Addgene 128833
pRSV-Rev	Kind gift from Gustavo Mostolavsky lab (Boston University School of Medicine, USA)	N/A
pMDLg/pRRE	Kind gift from Gustavo Mostolavsky lab (Boston University School of Medicine, USA)	N/A
pMD2.G	Kind gift from Gustavo Mostolavsky lab (Boston University School of Medicine, USA)	N/A
pHAGE zsGreen	Kind gift from Gustavo Mostolavsky lab (Boston University School of Medicine, USA)	N/A

pHAGE tdTomato	Kind gift from Gustavo Mostolavsky lab (Boston University School of Medicine, USA)	N/A
pHAGE TagBFP	Kind gift from Gustavo Mostolavsky lab (Boston University School of Medicine, USA)	N/A
Software and algorithms		
FlowJo	FlowJo, LLC	https://www.flowjo.com/
ZEN software	Zeiss	https://www.zeiss.com/microscopy/int/products/microscope-software/zen-lite.html
Prism8	GraphPad Inc.	https://www.graphpad.com/scientific-software/prism/
ImageJ	NIH, USA	https://imagej.nih.gov/ij/
CellSens Entry	Olympus	https://www.olympus-lifescience.com/en/software/cellsens/
10X Genomics CellRanger 7.0	10X Genomics Inc.	https://support.10xgenomics.com/single-cell-gene-expression/software/downloads/latest
Seurat R package v3.2.2	Satija Lab, USA	https://satijalab.org/seurat/
AUCell R package v1.8	Bioconductor project, USA	https://bioconductor.org/packages/release/bioc/html/AUCell.html
UTAP	Bioinformatics unit, Weizmann Institute of Science, Israel	https://utap.readthedocs.io/en/latest/
DESeq2.0	Bioconductor project, USA	https://bioconductor.org/packages/release/bioc/html/DESeq2.html
IGV	Broad Institute, USA	https://software.broadinstitute.org/software/igv/
Other		

PVDF filter 0.22 µm	Millipore	SLGV033RS
35mm glass bottom dishes	In Vitro Scientific	D35201.5N
0.22 µM filter	Nalgene	565-0020
AggreWell 24-well plate 400	STEMCELL Technologies	34415
AggreWell 24-well plate 800	STEMCELL Technologies	34815
Anti-adherent rinsing solution	STEMCELL Technologies	07010
6-well cell suspension non adherent culture plate	Greiner Bio	657185
LSM 700 inverted confocal microscope	Zeiss	N/A
Shaker (placed inside tissue culture incubator)	Thermo Scientific	88881102, 88881123
Electronic controller unit and gas mixing box for roller culture system	Aguilera-Castrejon et al., 2021	Hanna lab model 1 and 1.2 (assembled by Arad Technologies Ltd)
Roller Culture Incubator	Cullum Starr Ltd.	BTC Precision Incubator